FINITE ELEMENT METHOD IN APPLICATION TO PLANE STRESS PROBLEMS

by

BIJAYA C. MAHAPATRA
B.Tech (Hons), I.I.T., Kharagpur, India, Feb., 1964

A THESIS SUBMITTED IN PARTIAL FULFILMENT OF
THE REQUIREMENTS FOR THE DEGREE OF

MASTER OF APPLIED SCIENCE

in the Department

of

CIVIL ENGINEERING

We accept this thesis as conforming
to the required standard

THE UNIVERSITY OF BRITISH COLUMBIA

September, 1967.

In presenting this thesis in partial fulfilment of the requirements for an advanced degree at the University of British Columbia, I agree that the Library shall make it freely available for reference and Study. I further agree that permission for extensive copying of this thesis for scholarly purposes may be granted by the Head of my Department or by his representatives. It is understood that copying or publication of this thesis for financial gain shall not be allowed without my written permission.

Department of Civil Engineering

The University of British Columbia
Vancouver 8, Canada

Date September 1967

ABSTRACT

Framework cells and no-bar cells are used for solving plane stress problems by the Finite Element Method of Analysis and the results obtained by using the two types of cells are compared with the elasticity solution in two specific examples. The precision of the Finite Element Method is tested at different values of the Poisson's ratio of the material.

The stresses found by the Finite Element Method are calculated in two ways: from the corner forces and the corner displacements, and the quality of the results employing the methods is compared.

The precision of the results obtained with the bar cells has been found consistently better than with the no-bar cells. Comparable precision has been observed in the stresses found from the corner forces and the corner displacements.

ACKNOWLEDGEMENT

The writer is greatly indebted to Professor A. Hrennikoff for his invaluable guidance in the preparation of the thesis.

The writer wishes also to express his gratitude to Dr. Bülent Övünç and Mr. K.M. Agrawal for many valuable suggestions. Thanks are also due to the U.B.C. Computing Centre for free use of the computer.

INDEX

INTRODUCTION

The analytic solution of plane stress problems involves biharmonic equation subject to given boundary conditions. Unfortunately, however, selection of proper stress function, satisfying both the differential equation and the boundary conditions, is rarely possible and so it is very seldom that the problems can be solved exactly.

An ingenious method of solution was, however, introduced by Prof. Hrennikoff in 1941[1]*. The method consists of replacing the plate under consideration with a plane framework consisting of bar units or cells. The cells have a certain definite repreating pattern and are joined to each other at the corners. The external outline of the framework must conform to the outline of the given plate, and the framework must carry exactly the same forces and in the same locations as the plate. The bars have the same modulus of elasticity as the prototype and they must possess some appropriate cross-sectional areas, determined from the condition that the framework deforms in the same manner as the plate when placed in an arbitrary uniform stress field.

The use of the framework method requires the knowledge of a relationship between the corner forces and the corner displacements. If one of the corners of a cell is given unit displacement in the direction of one of the co-ordinate axes x or y, while the other corners are held in position, the x and y components of the corner forces required to hold the cell in the deformed state are called the "distribution factors" or "stiffness coefficients" of the cell. The distribution factors corresponding to

---

* Numbers signify the references, listed in the Bibliography

displacements of all corners, both in x and y directions, are arranged in the form of a matrix called the "stiffness matrix of the cell".

The model obtained by replacing the plate with elastic finite cells is highly indeterminate and its solution involves numerous linear simultaneous equations. Originally, the solution was achieved in a laborious way by the relaxation method. Subsequent introduction of digital computers drastically reduced the labor of computation.

Cells not involving bars have been also proposed. Unlike the framework cells the no-bar cells cannot be constructed physically, but like their framework counterpart, they allow one to obtain a set of distribution factors which may be used in the solution of plane stress problems. It is desirable to compare both the bar cell and the no-bar cell solutions with the elasticity solutions, where such are available.

The distribution factors, for both types of cells are functions of the Poisson's ratio of the material. The effect of the Poisson's ratio on the precision of the solution is also examined.

The plate stresses in the Finite Element solution are found in two ways: from the nodal concentrations and from the joint displacements. The quality of the two results is compared.

DERIVATION OF STIFFNESS MATRICES

2.1 BAR TYPE CELLS

Different patterns of bar type cells and determination of their parameters have been discussed in ref. 1 and 2. However, it is felt desirable to repeat parts of this discussion in application to rectangular cells in the present work.

2.2 RECTANGULAR PATTERN WITH AUXILIARY MEMBERS

This pattern is applicable to any arbitrary value of Poisson's ratio. It also allows one to use different sizes of cells in the same problem.

Consider a rectangular isotropic plate of uniform thickness (fig. 1a). The corresponding framework cell is shown in fig. 1b.

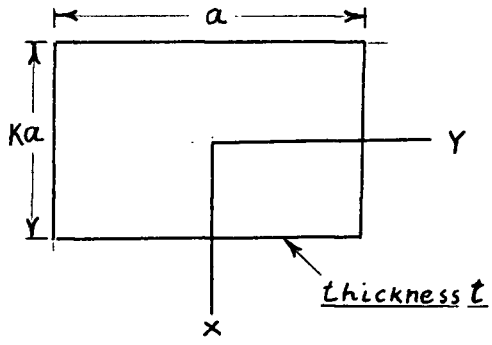

Fig. 1a

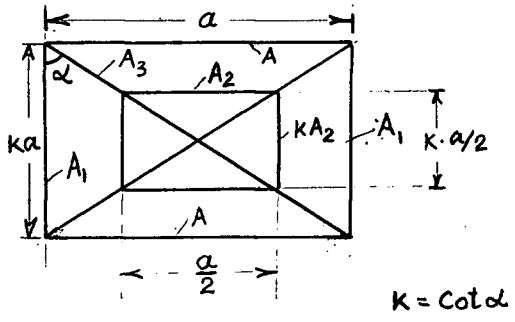

Fig. 1b

By an arbitrary assumption, the inner rectangle has dimensions half as great as those of the outer rectangle; the diagonals pass over each other at the centre without being connected. The external forces are assumed to be applied only at the main joints, and not at the joints of the inner rectangle. The deformability of the framework is judged on the basis of displacements of the main joints only, while the inner rectangles are viewed simply as an internal mechanism insuring proper deformability of the framework as described by the main joints.

2.2 RECTANGULAR PATTERN WITH AUXILIARY MEMBERS (cont'd)

The cell has five kinds of bar members: two kinds of outer bars, two of inner bars, and one of diagonal bars, assumed to possess the same area on the full length. However, it has been demonstrated[1] that such a cell can have the maximum of four independent characteristics, and so the area of the vertical bars of the inner rectangle is assigned at will, the area k times the one of the inner horizontal bar, i.e. kA_2.

It is easy to see that under all conditions, the opposite sides of the inner rectangle are stressed equally. This follows from conditions of equilibrium of the four joints of the inner rectangle.

Thus at joint ⑧ , Fig. 2

$$S_2^1 \sin\alpha = S_2 \cos\alpha$$

and at joint ⑥

$$S_2^1 \sin\alpha = S_2^* \cos\alpha$$

Therefore $S_2^1 = S_2 \cot\alpha = kS_2$)
and $S_2 = S_2^*$) — (1)

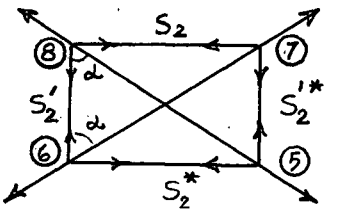

Fig. 2

Similarly considering the equilibrium of joints ⑤ and ⑦ one gets $S_2^1 = S_2^{1*}$ which shows that the bars on the opposite sides of the inner rectangle are stressed equally under all circumstances.

The four independent parameters A, A_1, A_2, and A_3 of the cell must be determined from the conditions of equal deformability with the plate in an arbitrary uniform stress field.

2.2 RECTANGULAR PATTERN WITH AUXILIARY MEMBERS (cont'd)

A general condition of uniform stress is achieved by combination of the following three types of uniform stress states:

$$\left.\begin{array}{llll} \sigma_x & , & \sigma_y = \tau_{xy} = 0 \\ \sigma_y & , & \sigma_x = \tau_{xy} = 0 \\ \tau_{xy} & , & \sigma_x = \sigma_y = 0 \end{array}\right\} \qquad (2)$$

It is more convenient, however, to make use of the following three strain conditions which lead to the same result as (2):

$$\left.\begin{array}{llll} \epsilon_x & , & \epsilon_y = \gamma_{xy} = 0 \\ \epsilon_y & , & \epsilon_x = \gamma_{xy} = 0 \\ \gamma_{xy} & , & \epsilon_x = \epsilon_y = 0 \end{array}\right\} \qquad (3)$$

CONDITION 1 $\quad \epsilon_x \; ; \epsilon_y = \gamma_{xy} = 0$

Uniform stresses p_1 and μp_1 are applied in x and y directions respectively (fig. 3).

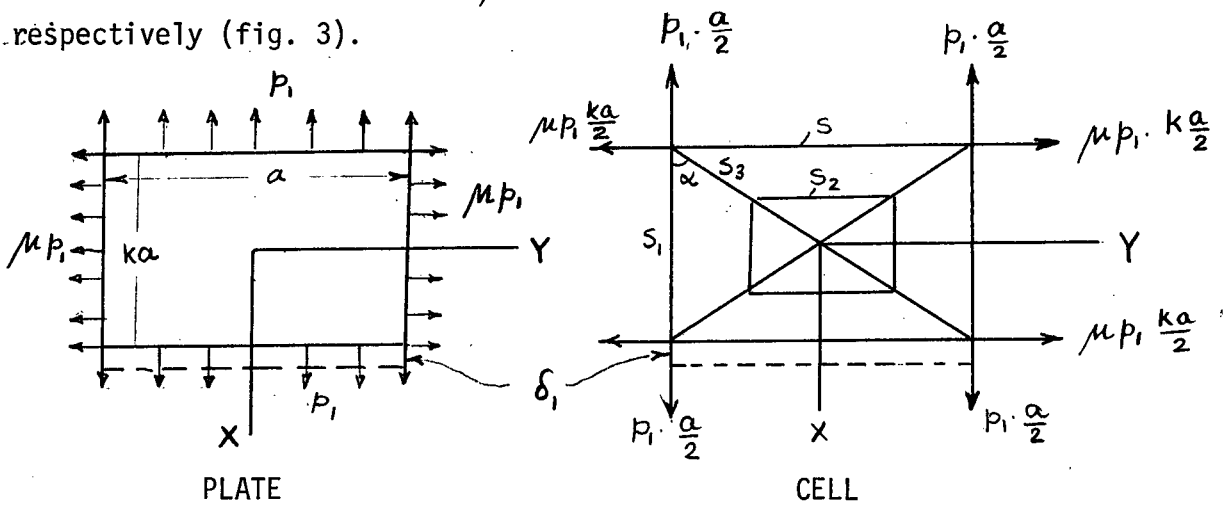

Fig. 3

2.2 RECTANGULAR PATTERN WITH AUXILIARY MEMBERS (cont'd)

Since there is no deformation in horizontal bars

$$S = 0 \qquad \text{and} \qquad S_1 = \frac{A_1 E}{ka} \cdot \delta_1 \tag{4}$$

where $\delta_1 = \frac{p_1}{tE} \cdot (1-\mu^2) \cdot k\alpha$

Transferring the edge stresses to corners by simple statics and analyzing an outside corner of the cell, one gets:

$$S_3 = \mu p_1 \cdot \frac{k\alpha}{2} \cdot \operatorname{cosec}\alpha$$

$$\text{and} \quad S_1 = p_1 \frac{\alpha}{2} - S_3 \cdot \cos\alpha = p_1 \cdot \frac{\alpha}{2}(1-\mu k^2) \tag{5}$$

Finally, equating (4) and (5)

$$A_1 = \frac{1-\mu k^2}{2(1-\mu^2)} \cdot \alpha t \tag{6}$$

CONDITION 2 ϵ_Y ; $\epsilon_x = \gamma_{xy} = 0$

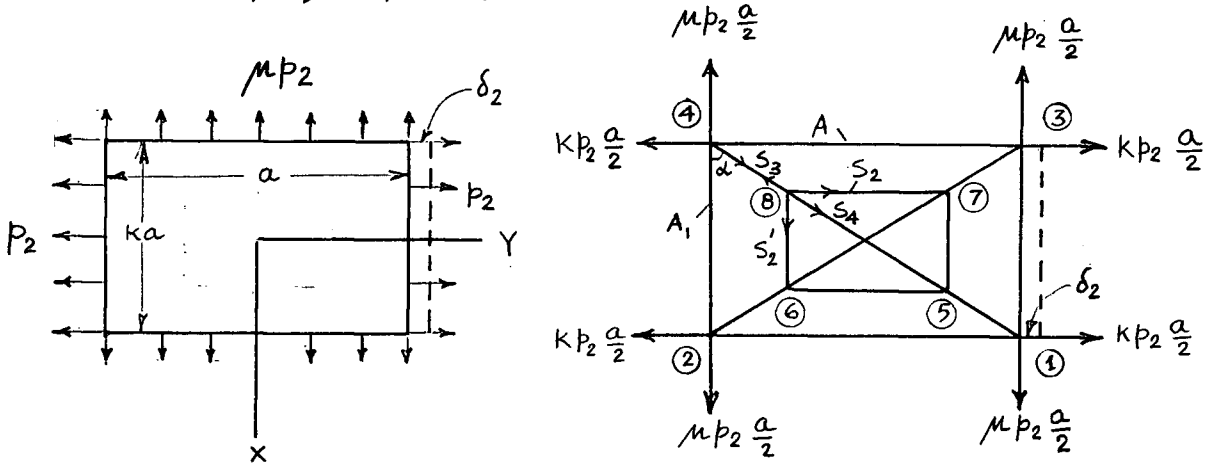

Fig. 4

This condition is analogous to Condition 1, carrying out the analysis in a similar manner, one gets:

$$A = \frac{k^2-\mu}{2k(1-\mu^2)} \cdot \alpha t \tag{7}$$

2.2 RECTANGULAR PATTERN WITH AUXILIARY MEMBERS (cont'd)

CONDITION 3

Pure shear condition is assumed as shown in Fig. 5.

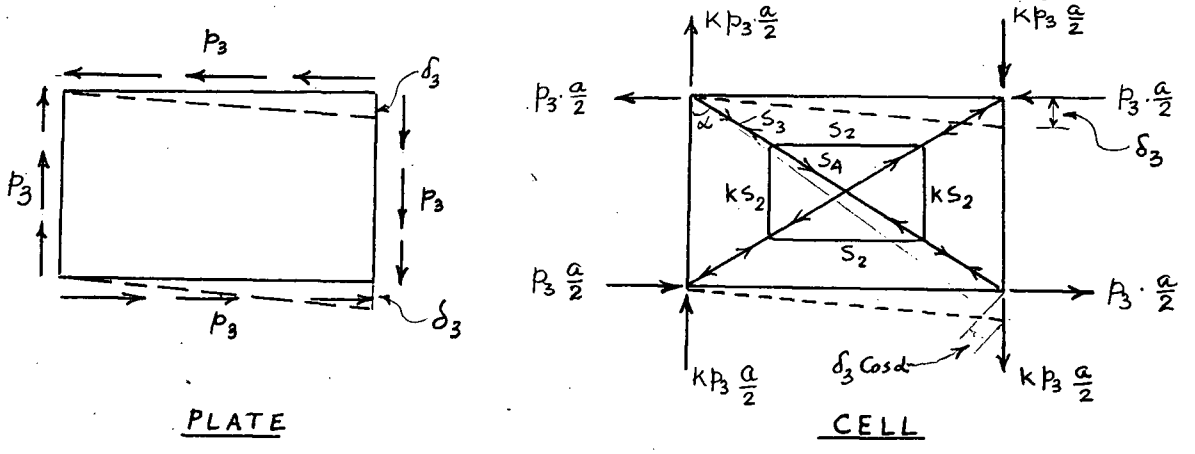

Fig. 5

From the deformability conditions (Fig. 5), it follows that the side members are unstressed while the outer parts of the diagonals are equally stressed with tension in one diagonal and compression in the other.

i. e. $S_3 = P_3 \cdot \frac{a}{2}\sqrt{1+K^2}$ tension and $S_3' = P_3 \frac{a}{2}\sqrt{1+K^2}$ comp. (8)

The equality of the displacements of the corners ① and ③ of the rectangle leads to equality of deformations of the two diagonals, one in tension, the other in compression by the amount $\delta_3 \cos\alpha$.

The antisymmetry of the loading condition demands that the stresses in the opposite sides of the inner rectangle must be equal and opposite. But, according to the statement of equation (1), they must also be equally stressed, thus the sides of the inner rectangle, in condition 3, must remain unstressed. i.e $S_2 = KS_2 = 0$.

2.2 RECTANGULAR PATTERN WITH AUXILIARY MEMBERS (cont'd)

With stresses S_2, being zero, the diagonals are stressed with the same stress on their full length and the change in length of the diagonal

$$= S_3 . a \frac{\sqrt{1+K^2}}{A_3 E} \qquad (9)$$

substituting the value of S_3 from (8) and equating equation (9) to $\delta_3 \cos\alpha$ one gets:

$$A_3 = \frac{at}{4(1+\mu)\sin^2\alpha \cdot \cos\alpha} \qquad (10)$$

To evaluate the area A_2, apply Condition 2 (Fig. 4) again.

Consider the inner rectangle:

Unit strain in the horizontal bar = $S_2 / A_2 E$ (11)

Unit strain in the vertical bar = $S_2' / K A_2 E$ (12)

But $S_2^1 = KS_2$ from (1)

Thus, from (11) and (12), the unit strains in the horizontal and vertical bars are equal. Since the load is symmetrical about both axes, the inner rectangle remains a geometrically similar rectangle after deformation.

i.e.: Unit strain in side members: = Unit strain in diagonals.

i.e.: $\frac{S_2}{A_2 E} = \frac{S_4}{A_3 E}$ OR $S_2 = \frac{A_2}{A_3} . S_4$ (13)

consider the equilibrium of joint ④:

2.2 RECTANGULAR PATTERN WITH AUXILIARY MEMBERS (cont'd)

$$S_3 \cos\alpha = \mu p_2 \cdot \frac{a}{2} \qquad \text{or} \qquad S_3 = \frac{\mu p_2 a}{2\cos\alpha} \tag{14}$$

Similarly, from equilibrium of Joint (8)

$$S_3 = S_4 + S_2' \cos\alpha + S_2 \sin\alpha = S_4 + S_2\sqrt{1+k^2} \tag{15}$$

From (13), (14), and (15)

$$\frac{\mu p_2 a}{\cos\alpha} = S_4 + \frac{A_2}{A_3} S_4 \sqrt{1+k^2} = S_4\left[1 + \frac{A_2}{A_3}\sqrt{1+k^2}\right]$$

$$\text{or} \qquad S_4 = \frac{\mu p_2 a}{2\cos\alpha}\left[\frac{1}{1+\frac{A_2}{A_3}\sqrt{1+k^2}}\right] \tag{16}$$

The total elongation of the diagonal member

$$= \frac{S_3 + S_4}{2} \times \frac{a\sqrt{1+k^2}}{A_3 E} = \delta_2 \sin\alpha$$

$$\text{Where} \quad \delta_2 = \frac{p_2 a}{Et}(1-\mu^2)$$

i.e. $$S_3 + S_4 = 2 \cdot \frac{p_2}{t}(1-\mu^2)\sin^2\alpha \cdot A_3$$

Substituting the value of S_3 from (14) in the above equation, one gets:

$$S_4 = \frac{p_2 a}{2\cos\alpha} \cdot (1-2\mu) \tag{17}$$

Finally, equating (16) and (17) and substituting the value of A_3 from (10):

$$A_2 = \frac{(3\mu-1)}{2(1+\mu)(1-2\mu)\sin 2\alpha} \cdot at$$

2.3 RIGIDITY OF THE CELL

It is necessary to see that the cell has enough bar members in relation to the number of joints to behave as a rigid structure. The cell has 14 members and 8 joints, not counting the points of intersection of the diagonals. In statically determinate rigid structures, the numbers

2.3 RIGIDITY OF THE CELL (cont'd)

of bars (b) and joints (j) are related by the equation of $b = 2j-3$. Hence, in the present case, the number of bars required = $2 \times 8 - 3 = 13$ which is one less than the number of bars present. The cell is, therefore, indeterminate and is obviously rigid.

The cell may become non-rigid in special circumstances. Examination of the expressions for A and A_1 shows that the main horizontal bar becomes zero when $k^2 - \mu = 0$, i.e.: $k = \sqrt{\mu}$. Similarly, the vertical bar vanishes when $k = 1/\sqrt{\mu}$. Both these conditions signify that if the ratio of the shorter side to the longer side equals $\sqrt{\mu}$, the area of the longer bar becomes zero. The total number of bars in the cell then becomes 12 making the structure non-rigid. A model consisting of such cells may still perform adequately in conditions of uniform stress but it becomes a mechanism when the stress is no longer uniform as is the case in all practical problems. The conclusion is that the cell with a side ratio of $\sqrt{\mu}$ may not be permitted.

The area A_3 of the diagonal can never be zero. The areas A_2 and kA_2 of the auxiliary bars become zero only when $\mu = 1/3$. Then the mid-length hinges on the diagonals disappear and the cell reduces to that of a simple rectangular pattern maintaining its rigidity.

The cell may become structurally unstable under compressive stress, in view of the absence of elastic restraint to rotation of the inner rectangle about an axis perpendicular to the plane of the framework. However, this does not affect the calculation of bar stresses since the model is not used for investigation of stability.

2.3 RIGIDITY OF THE CELL (cont'd)

As μ varies between the limits 1/2 and o, A_2 changes all way from + infinity through zero to a negative value. The area A becomes negative when $\kappa < \sqrt{\mu}$. Similarly, the area A_1 becomes negative for $\kappa > 1/\sqrt{\mu}$. Negative values of A, A_1 or A_2 make it impossible to construct a physical model of the cell but this does not affect its applicability in calculations.

2.4 STIFFNESS COEFFICIENTS FOR THE CELL

Calculation of distribution factors, after obtaining the areas of the bars, is a matter of ordinary structural analysis. However, the easiest way of obtaining them is by the use of an auxiliary condition in combination with the three main conditions discussed above.

AUXILIARY CONDITION - 4

The cell is subjected to a state of deformation in which one of its main vertical members is lengthened and the other shortened by the amount $2\delta_4$. (Fig. 6).

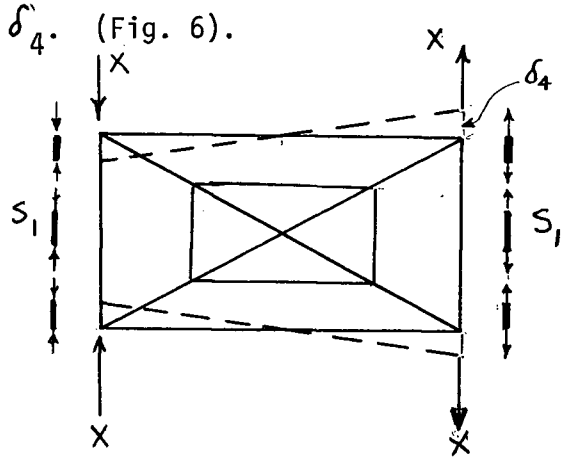

Fig. 6

It follows from antisymmetry of the stress condition about the vertical axis that all bars other than the two main vertical members remain unstressed. The stresses in the vertical sidebars,

2.4 STIFFNESS COEFFICIENTS FOR THE CELL (cont'd)

and corner forces equal to them, are given by the equation:

$$X = S_1 = \frac{2A_1E}{ka}\delta_4 = \frac{1-\mu k^2}{(1-\mu^2)k} Et\ \delta_4$$

It should be noted that in the previous three conditions, the corner forces were obtained from the plate stresses and not from the bar stresses as is done in the Condition 4.

Before combining the three conditions to produce unit displacement of any corner, it is necessary to demonstrate the nomenclature for the stiffness coefficients of the cell.

The eight directions of displacement of the cell corners are shown in Fig. 7(a) and the eight corner forces corresponding to unit displacement in direction 1 are shown in Fig. 7(b).

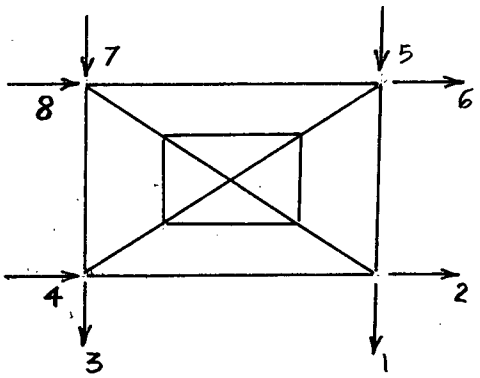

Fig. 7(a)

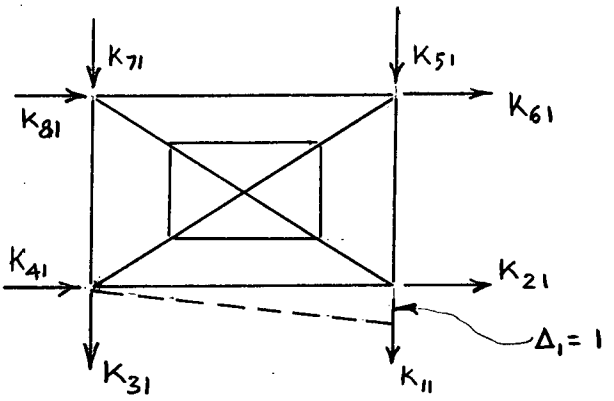

Fig. 7(b)

In general, K_{ij} = Force required in the direction i to produce a unit displacement in the direction j, in the absence of all other displacements.

The relationship between the corner forces and the corner displacement for a quadrilateral cell may then be written by the matrix equation (18).

2.4 STIFFNESS COEFFICIENTS FOR THE CELL (cont'd)

$$\begin{Bmatrix} F_1 \\ F_2 \\ F_3 \\ F_4 \\ F_5 \\ F_6 \\ F_7 \\ F_8 \end{Bmatrix} = \begin{bmatrix} k_{11} & k_{12} & k_{13} & k_{14} & k_{15} & k_{16} & k_{17} & k_{18} \\ k_{21} & k_{22} & k_{23} & k_{24} & k_{25} & k_{26} & k_{27} & k_{28} \\ k_{31} & k_{32} & k_{33} & k_{34} & k_{35} & k_{36} & k_{37} & k_{38} \\ k_{41} & k_{42} & k_{43} & k_{44} & k_{45} & k_{46} & k_{47} & k_{48} \\ k_{51} & k_{52} & k_{53} & k_{54} & k_{55} & k_{56} & k_{57} & k_{58} \\ k_{61} & k_{62} & k_{63} & k_{64} & k_{65} & k_{66} & k_{67} & k_{68} \\ k_{71} & k_{72} & k_{73} & k_{74} & k_{75} & k_{76} & k_{77} & k_{78} \\ k_{81} & k_{82} & k_{83} & k_{84} & k_{85} & k_{86} & k_{87} & k_{88} \end{bmatrix} \times \begin{Bmatrix} \Delta_1 \\ \Delta_2 \\ \Delta_3 \\ \Delta_4 \\ \Delta_5 \\ \Delta_6 \\ \Delta_7 \\ \Delta_8 \end{Bmatrix} \qquad (18)$$

The eight corner forces corresponding to any one of the main corner displacements may be found directly by moving the corner in question, but they are more conveniently determined by combining the several basic conditions analyzed above. Not all the conditions need to be used to produce the unit displacement of a particular corner. For example, to obtain a unit displacement in x direction of corner ①, (Δ_1=1), only three conditions are used (Fig. 8). The distribution factors are obtained by adding up the corner forces of individual conditions (Figs. 3, 5, and 6) with the values of "p"s replaced by corresponding δ values expressed in terms of Δ_1 (Fig. 8).

2.4 STIFFNESS COEFFICIENTS FOR THE CELL (cont'd)

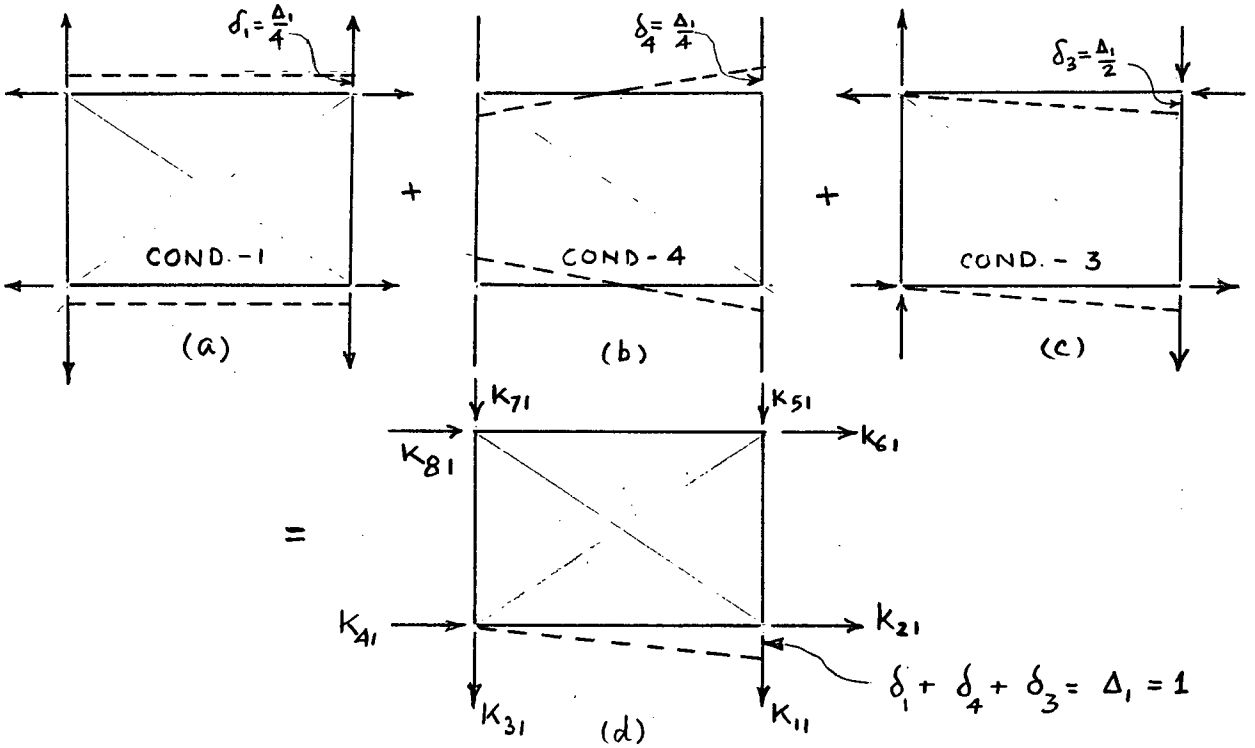

Fig. 8

The eight forces of figure 8(d) represent the elements of Column 1 of the stiffness matrix (k) in equation (18).

A similar set of eight forces can be obtained by giving unit displacement to corner (1) in the y direction. The distribution factors corresponding to unit displacement of corner (1) in x and y directions are summarized below in Table 1:

TABLE 1

Corner (1) Unit Displacement in x Direction		Corner (1) Unit Displacement in y Direction	
k_{11} =	$\frac{4 + k^2(1-3\mu)}{8k(1-\mu^2)} Et$	k_{12} =	$\frac{Et}{8(1-\mu)}$
k_{21} =	$\frac{Et}{8(1-\mu)}$	k_{22} =	$\frac{1 - 3\mu + 4k^2}{8k(1-\mu^2)} Et$

2.4 STIFFNESS COEFFICIENTS FOR THE CELL (cont'd)

TABLE 1 (cont'd)

Corner (1) Unit Displacement in x Direction	Corner (1) Unit Displacement in y Direction
$k_{31} = -\frac{(1-3\mu)k}{8(1-\mu^2)}Et$	$k_{32} = -\frac{(1-3\mu)}{8(1-\mu^2)}Et$
$k_{41} = \frac{1-3\mu}{8(1-\mu^2)}Et$	$k_{42} = \frac{1+\mu-4k^2}{8k(1-\mu^2)}Et$
$k_{51} = \frac{-4+k^2(1+\mu)}{8k(1-\mu^2)}Et$	$k_{52} = \frac{1-3\mu}{8(1-\mu^2)}Et$
$k_{61} = -\frac{1-3\mu}{8(1-\mu^2)}Et$	$k_{62} = -\frac{1-3\mu}{8k(1-\mu^2)}Et$
$k_{71} = \frac{k}{8(-\mu)}Et$	$k_{72} = -\frac{Et}{8(1-\mu)}$
$k_{81} = -\frac{Et}{8(1-\mu)}$	$k_{82} = -\frac{Et}{8k(1-\mu)}$

The corner forces produced by the displacements of corners ②, ③, and ④ are numerically equal to the corresponding forces resulting from displacements of the joint ①, presented in Table 1, although some of them have opposite signs.

This correspondence and the signs are determined by inspection. The stiffnex matrix expressed in terms of the coefficients of Table 1 is given in equation (19).

$$[K]_{8x8} = \begin{bmatrix} k_{11} & k_{12} & k_{31} & k_{41} & k_{51} & k_{61} & k_{71} & k_{81} \\ k_{21} & k_{22} & k_{32} & k_{42} & k_{52} & k_{62} & k_{72} & k_{82} \\ k_{31} & k_{32} & k_{11} & -k_{21} & k_{71} & -k_{81} & k_{51} & -k_{61} \\ k_{41} & k_{42} & -k_{21} & k_{22} & -k_{72} & k_{82} & -k_{52} & k_{62} \\ k_{51} & k_{52} & k_{71} & -k_{72} & k_{11} & -k_{21} & k_{31} & -k_{41} \\ k_{61} & k_{62} & -k_{81} & k_{82} & -k_{21} & k_{22} & k_{32} & k_{42} \\ k_{71} & k_{72} & k_{51} & -k_{52} & k_{31} & k_{32} & k_{11} & k_{21} \\ k_{81} & k_{82} & -k_{61} & k_{62} & -k_{41} & k_{42} & k_{21} & k_{22} \end{bmatrix} \quad (19)$$

2.4 STIFFNESS COEFFICIENTS FOR THE CELL (cont'd)

Examination of the matrix (19) reveals that it is symmetrical about the main diagonal.

i.e.: $k_{ij} = k_{ji}$

This result is in agreement with Bett's reciprocal theorem.

2.5 NO-BAR CELL

Finite Element cells not made up of bars have also been proposed.[4] Their nature may be explained as follows:

Imagine a piece of rectangular plate placed in a stress field, preferably a simple case such as that of the uniform stress field (Fig. 9(a)). The deformation of the plate under this stress field is also shown in the figure.

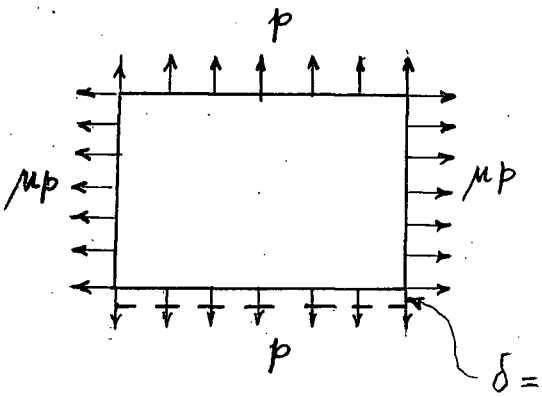

PLATE

Fig. 9(a)

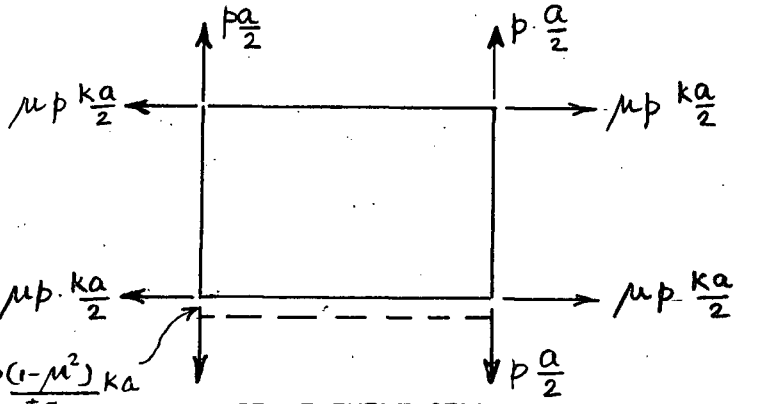

FINITE ELEMENT CELL

Fig. 9(b)

The stresses acting on the edges of the plate are assembled at the corners in a manner consistent with statics such as the one employed earlier in the framework cells (Fig. 3). A different method based on energy considerations may also be used for this purpose. The transfer of edge stresses to the corners transforms the piece of plate into a no-bar cell (Fig. 9(b)) to be used in the analysis. The cell must satisfy several

2.5 NO-BAR CELL (cont'd)

of such stress conditions. Proper combinations of these would result in single corner displacements and would allow one to determine the distribution factors.

A plate polygon of N-sides has 2N degrees of freedom of its corners as they move while the cell deforms under stress. Three of these displacements may be affected by rigid body movements without imposing any stresses on the cell. This leaves (2N-3) independent stress conditions required for derivation of stiffness matrix, irrespective of actual shape of the finite element. A rectangular cell thus demands five (2N-3=5) stress conditions for obtaining its stiffness matrix. Of these five, three must correspond to the uniform states of stress, i.e.: the same states as used for the bar type cells. The corner forces obtained for these three conditions are equally applicable for the present case since they were found from the plate prototype and not from the bar stresses as explained earlier.

The two extra conditions to be used now are shearless bending in the plane of the plate with stresses acting in x and y directions.

CONDITION - 4* - Bending with stresses acting in x Direction (Fig. 10(a)).

No stresses of any kind are present on the vertical sides of the element and no shear stresses on the horizontal sides.

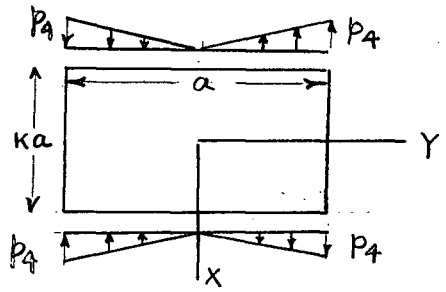

Fig. 10(a)

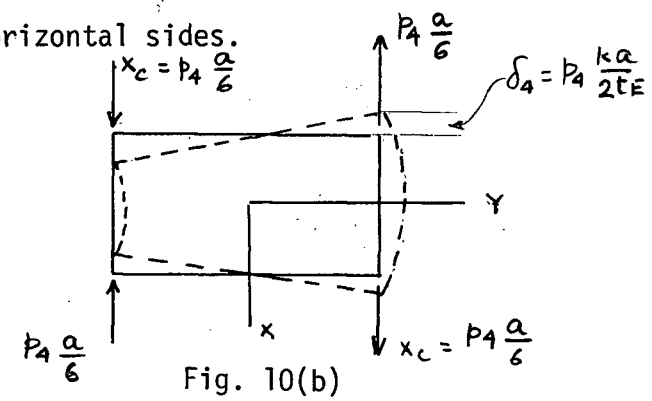

Fig. 10(b)

2.5 NO-BAR CELL (cont'd)

The corner forces for the cell (Fig. 10(b)) statically equivalent to the flexural stresses are found thus: $X_c.a = (\frac{2}{3}a) \times (P4\frac{a}{4})$

$$\text{OR: } X_c = p_4 \cdot \frac{a}{6}$$

CONDITION 5* - This condition is similar to Condition 4* with stresses acting in y direction (Fig. 11).

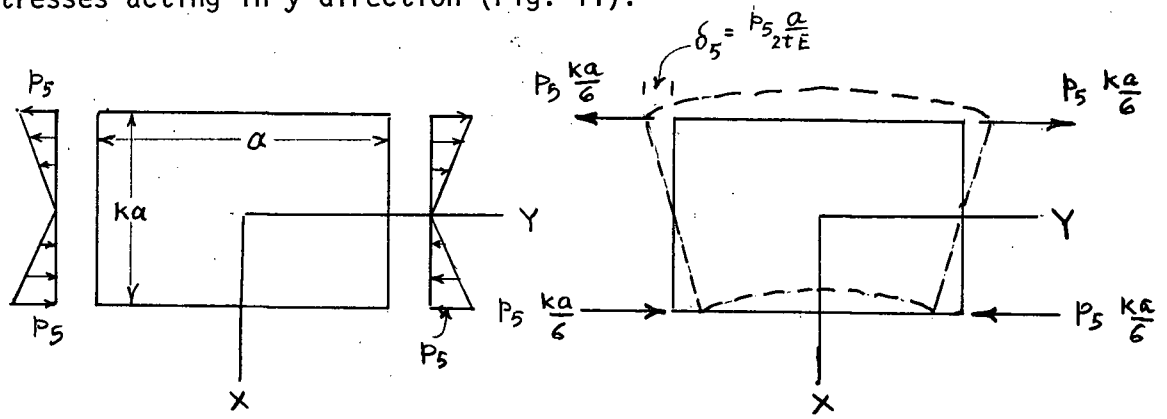

Fig. 11

2.6 STIFFNESS COEFFICIENTS OF THE NO-BAR CELL

Corner (1) is made to displace a unit distance $\Delta_1 = 1$ by combining the three conditions as shown in Fig. 12.

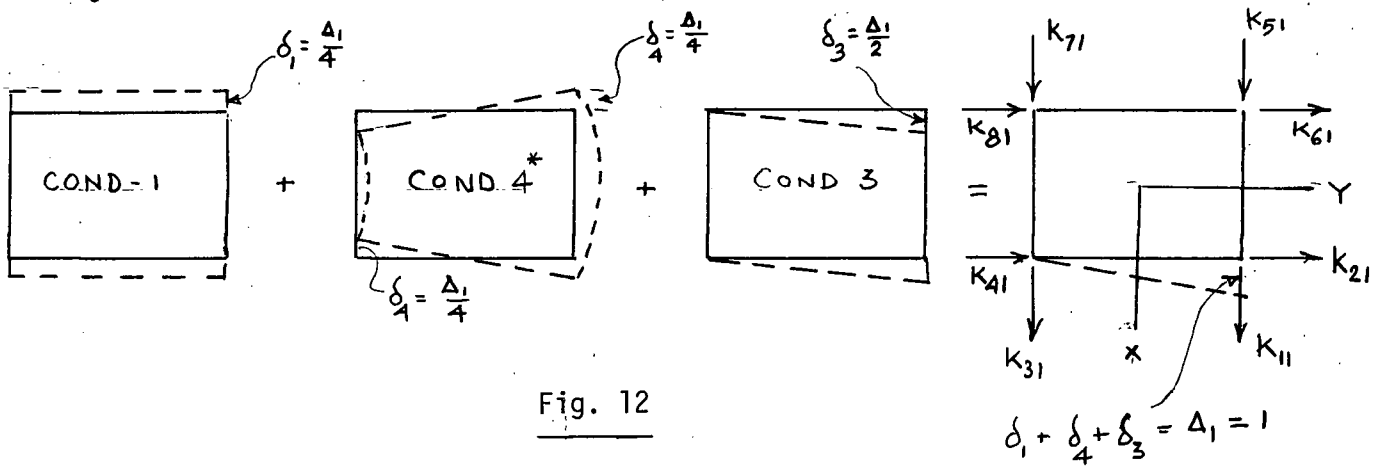

Fig. 12

2.6 STIFFNESS COEFFICIENTS OF THE NO-BAR CELL (cont'd)

The distribution factors are obtained by adding up the corresponding corner forces of the individual conditions as was done with the bar cells. The set of distribution factors corresponding to unit displacement of corner ① in direction 2 ($\Delta_2=1$) may be obtained in a similar manner from the three conditions 2, 3, and 5*. The results are summarized in Table 2.

TABLE 2

Corner (1) Unit Displacement in x Direction $_1=1$	Corner (1) Unit Displacement in y Direction $_2=1$
$k_{11} = \left[\frac{4-\mu^2}{12k(1-\mu^2)} + \frac{k}{8(1+\mu)}\right] Et$	$k_{12} = \frac{Et}{8(1-\mu)}$
$k_{21} = \frac{Et}{8(1-\mu)}$	$k_{22} = \left[\frac{(4-\mu^2)k}{12(1-\mu^2)} + \frac{1}{8k(1+\mu)}\right] Et$
$k_{31} = \left[\frac{2+\mu^2}{12k(1-\mu^2)} \quad \frac{k}{8(1+\mu)}\right] Et$	$k_{32} = -\frac{1-3\mu}{8(1-\mu^2)} Et$
$k_{41} = \frac{1-3\mu}{8(1-\mu^2)} Et$	$k_{42} = -\left[\frac{(4-\mu^2)k}{12(1-\mu^2)} - \frac{1}{8k(1+\mu)}\right] Et$
$k_{51} = -\left[\frac{4-\mu^2}{12k(1-\mu^2)} - \frac{k}{8(1+\mu)}\right] Et$	$k_{52} = \frac{(1-3\mu)}{8(1-\mu^2)} Et$
$k_{61} = -\frac{(1-3\mu)}{8(1-\mu^2)} Et$	$k_{62} = \left[\frac{(2+\mu^2)k}{12(1-\mu^2)} - \frac{1}{8k(1+\mu)}\right] Et$
$k_{71} = -\left[\frac{2+\mu^2}{12k(1-\mu^2)} + \frac{k}{8(1+\mu)}\right] Et$	$k_{72} = -\frac{Et}{8(1-\mu)}$
$k_{81} = -\frac{Et}{8(1-\mu)}$	$k_{82} = \left[\frac{(2+\mu^2)k}{12(1-\mu^2)} + \frac{1}{8k(1+\mu)}\right] Et$

The distribution factors corresponding to unit displacements of corners (2), (3) and (4) are obtained from Table 2 in the same way as for the bar type cell. Equation 19 is equally applicable in the present case.

The same set of distribution factors have been obtained from the energy consideration in Ref. 4.

2.7 SYMMETRY OF STIFFNESS MATRICES

The matrix formed of the coefficients of Table 2 like the matrix described earlier is symmetrical about the principal diagonal. Symmetry of the stiffness matrix of a cell made up of bars is the direct consequence of Betti's reciprocal theorem, since the framework cell is a real elastic structure and Betti's theorem is applicable to all linear elastic structures.

As to the no-bar cells, its stiffness matrix is always symmetrical when its terms are determined from the energy considerations, With its terms found by the Law of the Lever, as described above the matrix is symmetrical or unsymmetrical depending upon the cell itself being symmetrical or unsymmetrical. Thus the matrix is symmetrical for a rectangular cell and unsymmetrical for a cell in the form of a trapizoid.[3]

2.8 COMPARISON OF MATRICES

It is interesting to note that some of the corresponding terms in Tables 1 and 2 are equal and it is easy to see the reason for this peculiarity. The elements in Column 1 of Table 1 were obtained by combining the Condition 4 with Conditions 1 and 3 (Fig. 8). The corresponding elements in Table 2 were obtained by combining Condition 4* with the same conditions 1 and 3 (Fig. 12). Thus the contribution of the Conditions 1 and 3 to the two sets of distribution factors is the same. Condition 4 and Condition 4* have no corner forces in the y Direction, thus making the total corner forces in the y Direction equal for both types of cells. That is k_{21}, k_{41}, k_{61}, and k_{81} are the same for both. On the other hand, the Condition 4 and 4* contribute different corner forces in the x Direction thus making the distribution factors in the x Direction (k_{11}, k_{31}, k_{51}, and k_{71}) unequal for the two types of cells.

2.8 COMPARISON OF MATRICES (cont'd)

A similar reasoning shows that, the distribution factors of the Column 2 in x Direction are the same in both Tables.

2.9 SOLUTION OF PLATE MODEL BY FINITE ELEMENT METHOD

The plate under consideration is replaced by a model consisting of many cells of proper shape and size and is provided with the same boundary conditions and the loads "F" as the prototype. The solution of the model involves determination of all nodal displacements for which purpose the stiffness matrix (K) of the model is set up by the computer by combining the stiffness matrices (k) of the individual cells. The computer solves the system of simultaneous equations:

$$[K] \times \{\Delta\} = \{F\}$$

for the joint displacements $\{\Delta\}$ and knowing these finds the corner forces $\{f\}$ of the individual cells from the displacements $\{\delta\}$ of the cells.

Thus: $$\{f\} = [k] \times \{\delta\}$$

The plate stresses are subsequently calculated by dividing the nodal forces by the corresponding tributary areas equal to the product of the length or breadth of the cell and the thickness of the plate.

An alternative procedure of finding the stresses directly from the displacements is discussed in Chapter V.

EXAMPLES OF SOLUTION BY FINITE ELEMENT THEORY

Finite element solutions, making use of different matrices, procedures and values of Poisson's ratio are compared on two examples for which there exist rigorus elasticity solutions.

3.1 EXAMPLE 1

A thin semi-infinite plate is acted upon by a concentrated force P per unit thickness directed perpendicularly to the straight edge (Fig. 13)

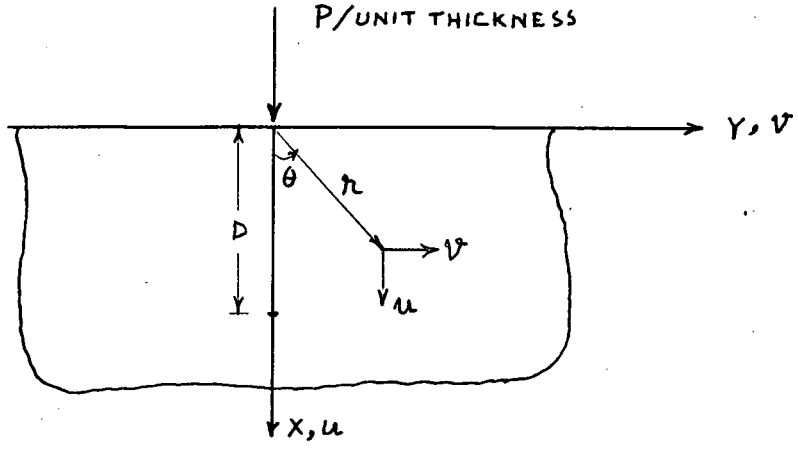

Fig. 13

The expressions for the displacements u and v in x and y Directions are[5]

$$u = -\frac{2P}{\pi E} \ln\left(\frac{r}{D}\right) - \frac{P}{\pi E} \sin^2\theta \,(1+\mu)$$

$$v = -(1-\mu)\frac{P}{\pi E}\theta + \frac{P}{\pi E} \sin\theta \cdot \cos\theta \,(1+\mu) \qquad (20)$$

The significance of the symbols is given in Fig. 13. D is the distance from the origin of a point on x-axis which is considered stationary.

3.1 EXAMPLE 1 (cont'd)

The expressions for stress are given by:

$$\sigma_x = -\frac{2P}{\pi x} \cdot \cos^4\theta$$

$$\sigma_Y = -\frac{2P}{\pi x} \cdot \sin^4\theta \qquad (21)$$

$$\tau_{xY} = -\frac{2P}{\pi x} \cdot \sin\theta \cdot \cos^3\theta$$

In view of the symmetry of the structure and the loading system it is sufficient to analyze one-half of the model which is assumed to consist of 12x6 cells of size (axa). The immovable point F is located at the bottom of the model. The boundary conditions are prescribed (Fig. 14) in terms of the known displacements along the boundary BCF, determined by

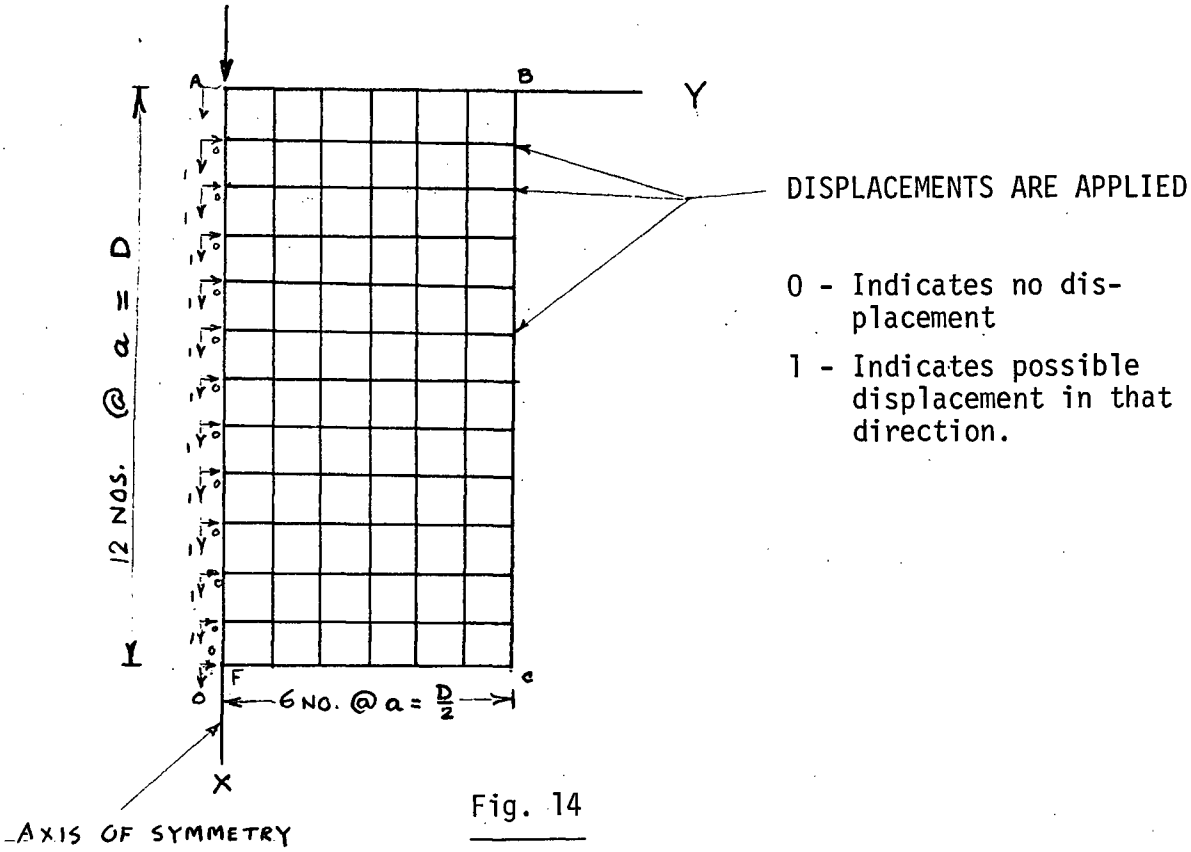

Fig. 14

3.1 EXAMPLE 1 (cont'd)

the elasticity equation (20). No horizontal displacements are present along the axis of symmetry AF.

The stresses and displacements at the nodal points along the x-axis are shown in Plate 1. The plate consists of several graphs presenting stresses and displacements along the x-axis for the values of Poisson's ratio μ = o.o, o.2 and o.4. Each graph contains three curves: the curve of stresses or displacements determined by elasticity solution and the two curves of the percentage deviations of the bar and no-bar models solutions from the elasticity values. At most of the points, the errors are below 10% and usually much below this figure, except where the function itself (stress or displacement) is very small. However, greater errors in σ_x are found at the node next to the point of application of the load P. The reason for this discrepancy is quite clear from the sign of the error and the nature of the true solution. At the point P the elasticity stress σ_x is infinite and at the adjacent node directly below P, it is very high retreating fast both ways to the left and to the right from the axes of symmetry. The nodal concentration in x Direction naturally reflects the mean stress σ_x over a certain adjacent area and this, of course, is smaller than the true stress on the axis of symmetry. The Finite Element Stress σ_x is thus numerically smaller than the true stress. The error of this type when the elasticity stress exceeds numerically the Finite Element stress is called negative. σ_y and τ_{xy} stresses on the x-axis are zero.

The high percentage error has a practical significance only when the values of the function (stresses or displacements) are themselves

3.1 EXAMPLE 1 (cont'd)

large and not when they are very small.

The results obtained at the joints near the applied load P can be made closer to the elasticity solution by using smaller rectangular cells joined to the bigger cells below by appropriate triangular elements. However, the results will be affected by the presence of the triangular cells, and the direct comparison of the precision of the finite element method with regard to stresses and deflections while using the rectangular bar and no-bar cells will be obscured.

In Plates 2 and 3 are presented the data pertaining to the Sections AA and BB similar to the ones of Plate 1. Here again, the results are much the same as in Plate 1, i.e.: the errors are reasonably small and consistently better with the bar cells.

3.2 EXAMPLE 2

In this example a point load is applied within an infinite plate (Fig. 15).

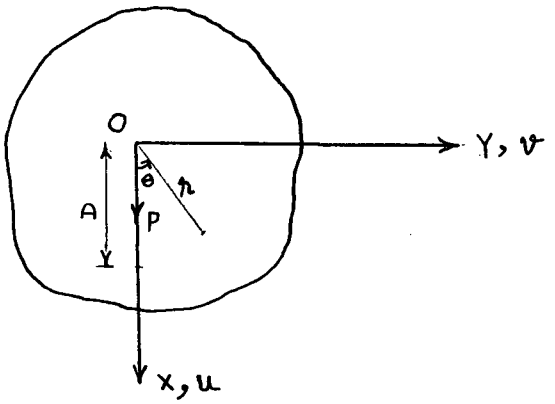

Fig. 15

The exact values of stresses and displacements are:

$$\sigma_x = \frac{P}{4\pi}\frac{\cos\theta}{r}\left[-(3+\mu) + 2(1+\mu)\sin^2\theta\right]$$
$$\sigma_Y = \frac{P}{4\pi}\frac{\cos\theta}{r}\left[(1-\mu) - 2(1+\mu)\sin^2\theta\right] \qquad (22)$$
$$\tau_{xY} = -\frac{P}{4\pi}\frac{\sin\theta}{r}\left[(1-\mu) + 2(1+\mu)\cos^2\theta\right]$$

3.2 EXAMPLE 2 (cont'd)

$$u = \frac{P}{4\pi E}\left[-(1+\mu)^2\sin^2\theta - (1+\mu)(3-\mu)\log\left(\frac{r}{D}\right)\right]$$

$$v = \frac{P}{4\pi E}(1+\mu)^2 \sin\theta \cdot \cos\theta \,. \qquad (23)$$

The significance of the terms in these equations is the same, and as in Example 1. D is again the distance from the origin of the point on the x-axis which is considered stationary. In view of the symmetry of the structure it is sufficient to analyze only one-quarter of the model which is assumed to consist of 12x6 cells of the size a x a. The immovable point on the x-axis is located at the bottom of the model. The boundary conditions for the model are prescribed in terms of its known displacements along BCF (Fig. 14), determined from equation (23), as in Example 1, with the exception that the y-displacements (v) along the y-axis AB are also specified to be zero.

The results obtained by the finite element theory are shown graphically in Plates 4, 5, and 6 in the same way as in the Example 1. The stresses and displacements at nodal points along x-axis are shown in Plate 4. Because of symmetry v and τ_{xy} have zero values along this axis. The values of u obtained by using both types of cells have an error less than 3%, but the results obtained with no-bar model are slightly better than the bar model. The values of σ_x obtained by using the bar model are much better than those obtained with the no-bar model. Both models give a high percentage error at the node next to the point of application of the load P, and the reason for this discrepancy has been explained in Example 1. σ_y values are sometimes better with the no-bar model and sometimes with the bar model.

3.2 EXAMPLE 2 (cont'd)

The stresses and displacements along the Sections AA and BB passing through the middle of the model are presented in the Plates 5 and 6. The results obtained with the bar model are consistently better than with the no-bar model.

3.3 DISCUSSION

The difference between the distribution factors of Table 1 (bar cell) and Table 2 (no-bar cell) is that the former are based on imitation of deformabilities of the prototype by the model in conditions of uniform stress, while in the latter, the model and the prototype are made to deform in the same manner not only under uniform stress, but also in conditions of shearless bending. For this reason, one might expect a greater accuracy of the no-bar cells. However, the results of the two examples do not confirm this expectation.

The plate stress distribution in practical engineering problems is never uniform. At the same time, the manner of deviation of the plate stress from uniformity is not likely to be that of shearless bending. Hence, from the theoretical point of view, the results obtained with the no-bar model need not necessarily be better than with the bar model. Actually, in the two given examples, the bar model was found to be superior to the other.

As the size of the mesh decreases, the stresses in the vicinity of the individual cells become more uniform and the results obtained by either type of cells should become more precise and in the limit should converge to the elasticity solution.[3] Therefore, the use of either type of cell appears quite proper in the Finite Element Method of Analysis, but the precision is expected to be better with the bar cells.

3.3 DISCUSSION (cont'd)

Although the shape of the cells in both examples was square, it is felt that the results obtained with oblong cells would not be much different as long as the ratio of the sides of the rectangles differs sufficiently from the relation $K = \sqrt{\mu}$.

ACCURACY OF FINITE ELEMENT METHOD AND POISSON'S RATIO

The precision of the results obtained by the Finite Element Method seems to depend on the value of the Poisson's ratio, and so it is desirable to study more closely this dependence. In the elasticity solution, the displacements are always functions of μ , but the stresses are influenced by μ only when the loads are applied within the area of the plate, as in example 2, and are independent of μ with the loads acting on the periphery of the area, as in Example 1. The distribution factors in the Finite Element Method depend on μ . Then one may expect that in the problems of the latter type the effect of μ on the stresses must somehow cancel out.

The effect of μ on the percentage error and displacements found by the Finite Element Method is demonstrated in Plates 7, 8, 9 and 10. The first two of these refer to the Example 1 and the last two refer to the Example 2. The exact values of the functions and the percentage errors are found at six nodes located on the lines 15-21 and 36-42 of Figure 17. Five values of μ ranging from 0.0 to 0.4 at an interval of 0.1, are used for the above purpose.

The Plates 7 and 8 show that in most cases the curves of percent error versus μ for stresses are linear. In some cases the errors change from positive to negative or vice versa. The percentage errors for displacements " u " do not change much with the change in μ . Their graphs are linear with small slopes in either direction. The displacements " v " have small absolute values at some of the joints under consideration resulting in a high percentage error by the Finite Element Method. The

curves of errors of ν at such points are not shown in the figure.

In Example 2, the formula (22) shows that

$$\frac{(\sigma)_{\mu_1} - (\sigma)_{\mu_2}}{\mu_1 - \mu_2} = f(r,\theta) \qquad (24)$$

where $f(r,\theta)$ is constant for any particular point and (σ) represents any one of the stress components σ_x, σ_y, and τ_{xy} at the same point for different values of μ. Equation (24) shows that the stresses at any point vary linearly with μ.

The percentage error of stresses at joints 17, 19, and 21 (Plate 9) vary almost linearly with the Poisson's Ratio and the amount of variation is significant as seen from the graphs, while for joints 38, 40, and 42 the variation is less significant. Like the previous example, the errors at times increase and at others decrease with increase of the Poisson's Ratio. The plots of percentage error of displacements versus μ are also nearly linear in most cases, although the amount of variation from the true values is very small.

No substantial difference is noticeable in this respect between the two examples in the first of which the true stresses are independent of the Poisson's Ratio, and in the second one are functions of it. The percentage errors in both examples are comparable.

DETERMINATION OF STRESSES FROM NODE DISPLACEMENTS

In Chapter 3, the Plate stresses were calculated from the nodal force concentrations. As an alternative procedure, they may also be found from the joint displacments.

Stresses at a point in terms of strain components are:

$$\sigma_x = \frac{E}{1-\mu^2}(\epsilon_x + \mu\epsilon_y)$$

$$\sigma_y = \frac{E}{1-\mu^2}(\mu\epsilon_x + \epsilon_y) \qquad (25)$$

$$\tau_{xy} = \frac{E}{2(1+\mu)}\gamma_{xy}$$

The strains may be evaluated in two different ways.

a) Consider an interior joint (5) in Fig. 16.

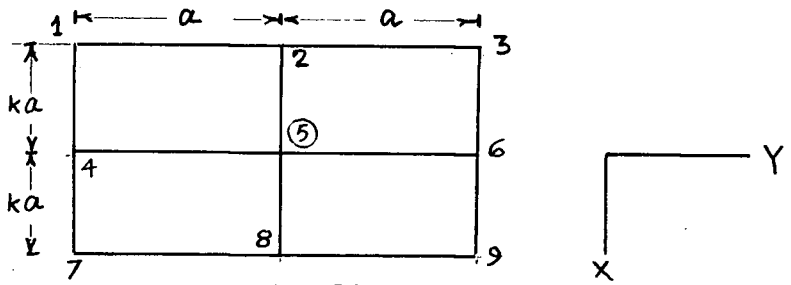

Fig. 16

The average strains at joint (5), in the simplest form, may be given in terms of its displacements of its adjacent joints, thus:

$$\epsilon_x = \frac{U_8 - U_2}{2ka}$$

$$\epsilon_y = \frac{V_6 - V_4}{2a} \qquad (26)$$

$$\gamma_{xy} = \left(\frac{U_6 - U_4}{2a} + \frac{V_8 - V_4}{2ka}\right)$$

where u and v are the displacements in x and y directions respectively. The subscript shows the corresponding joint. Substitution of equation (26) in (25) leads to:

$$\sigma_x = \frac{E}{1-\mu^2}\left[\frac{U_8 - U_2}{2ka} + \mu\,\frac{V_6 - V_4}{2a}\right]$$

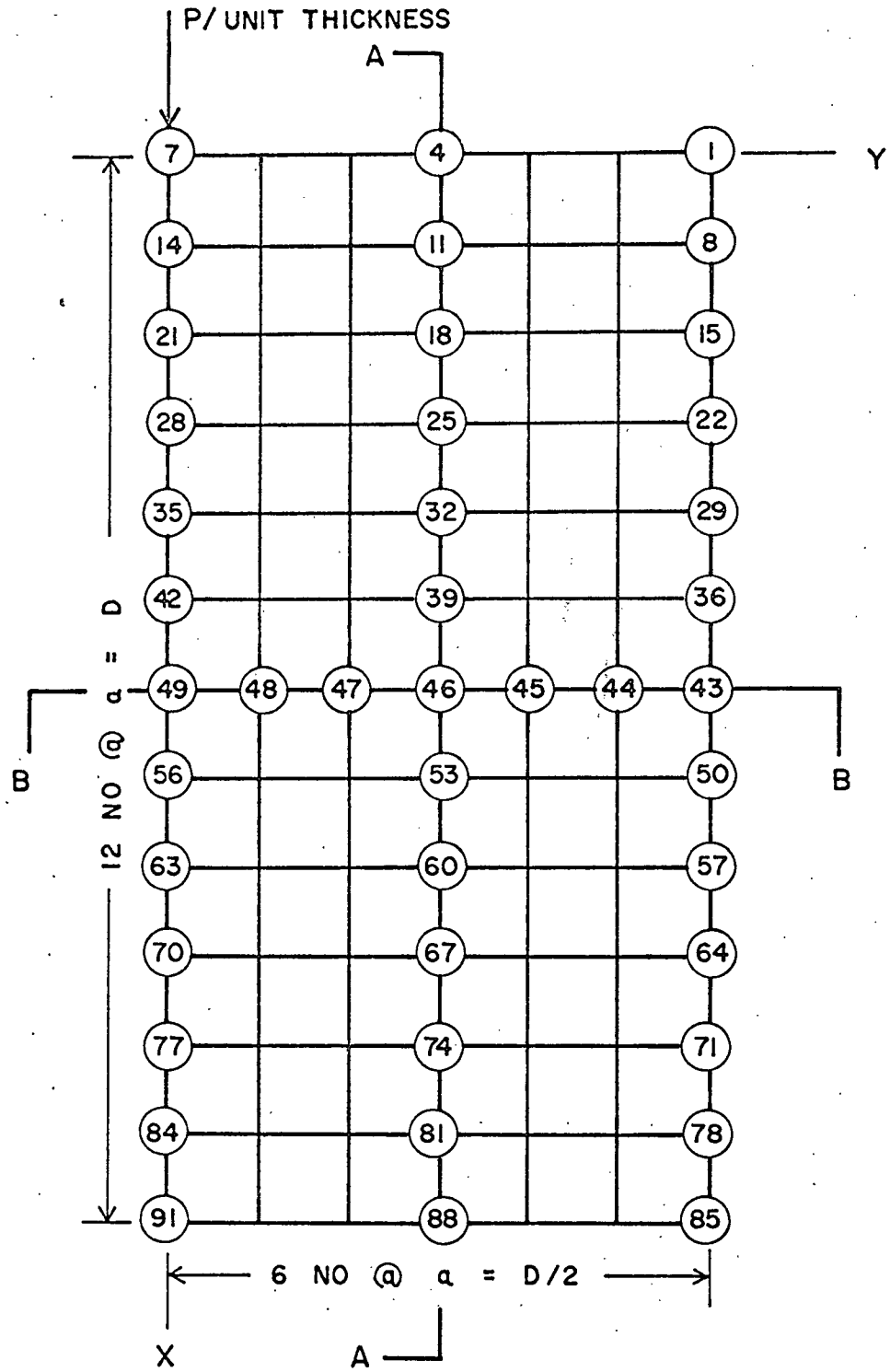

NUMBERING OF JOINTS AND SECTIONS ALONG WHICH STRESSES AND DISPLACEMENTS ARE COMPARED

FIG. 17

$$\sigma_Y = \frac{E}{1-\mu^2}\left[\frac{V_6 - V_4}{2a} + \mu\,\frac{U_8 - U_2}{2ka}\right]$$

$$\tau_{XY} = \frac{E}{2(1+\mu)}\left[\frac{U_6 - U_4}{2a} + \frac{V_8 - V_2}{2ka}\right] \qquad (27)$$

b) A more elaborate expression for the strains at the node 5 making use of the four surrounding cells, leads to the following expression.[3]

$$\sigma_X = \frac{E}{1-\mu^2}\left[\frac{U_8 - U_2}{2ka} + \mu\,\frac{2(V_6 - V_4) + (V_3 - V_1) + (V_9 - V_7)}{8a} + \mu^2\,\frac{2(U_7 - U_1) + (U_9 - U_3) + (U_8 - U_2)\times 2}{8ka}\right]$$

$$\sigma_Y = \frac{E}{1-\mu^2}\left[\frac{V_6 - V_4}{2a} + \mu\cdot\frac{2(U_8 - U_2) + (U_7 - U_1) + (U_9 - U_3)}{8ka} + \mu^2\,\frac{(V_9 - V_7) + (V_3 - V_1) + 2(V_6 - V_4)}{8a}\right] \qquad (28)$$

$$\tau_{XY} = \frac{E}{2(1+\mu)}\left[\frac{2(V_6 - V_4) + (U_3 - U_1) + (U_9 - U_7)}{8a} + \frac{2(V_8 - V_2) + (V_9 - V_3) + (V_7 - V_1)}{8ka}\right]$$

The no-bar model was used for comparison of stresses found by equations (27) and (28) in the Examples 1 and 2. At some nodal points, the results are better with equation (27) and at others with equation (28). The more elaborate formula appeared to have no extra precision of results over its more simple counterpart.

Stresses obtained from the corner forces and the nodal displacements (equation 28) were compared in accuracy for the bar and the no-bar models. The results are shown in Plates 11, 12, 13, and 14. The Plates consist of several figures each containing three curves showing the elasticity solution and the percentage error in stresses employing the two methods. The curves show that for the bar model the results are slightly better with the corner force, although the difference is

very small. For the no-bar model the results at some points are better with the corner forces while at the other points, they are better with the nodal displacements.

Thus, both the nodal force and the nodal displacement methods appear adequate for calculation of stresses, but the results obtained have not been extensive enough to allow one to form a definite conclusion as to the superiority of one method over the other.

CONCLUSIONS

Actual solution of examples shows that:

1. It is quite proper to use both the bar type and the no-bar type rectangular cells in the Finite Element Method of Analysis.

2. The precision of the values of stresses and displacements obtained with the bar model is better than with the no-bar model.

3. The accuracy of the Finite Element Method depends upon the property μ of the material. The nature of variation of the percentage error in stresses and displacements at any point is linear in μ in most cases.

4. No noticeable difference in the percentage error in stresses for different values of μ is observed between the two examples, in one of which the true stresses depend on μ and in the other do not.

5. The plate stresses may be calculated either by employing the nodal force concentrations or the joint displacements. The results obtained by the two methods are comparable in precision.

BIBLIOGRAPHY

1. A. Hrennikoff, "Solution of Problems of Elasticity by the Framework Method", Journal of Applied Mechanics, A.S.M.E., New York, Vol. 63, Dec. 1941.

2. A. Hrennikoff, "Framework Method and Its Technique for Solving Plane Stress Problems", Publications of International Association for Bridge and Structural Engineering, Zurich, Switzerland, Vol. 9-1949.

3. A. Hrennikoff, Mimeographed Notes On Plane Stress, in Course CE 551.

4. R.W. Clough, "The Finite ELement Method in Plane Stress Analysis", Proceedings of A.S.C.E. 2nd Conference on Electronic Computation, Pittishburgh, Sept., 1960.

5. Timoshenko and Goodier, "Theory of Elasticity", McGraw Hill Book Company.

RESULTS AT NODAL POINTS ALONG X-AXIS

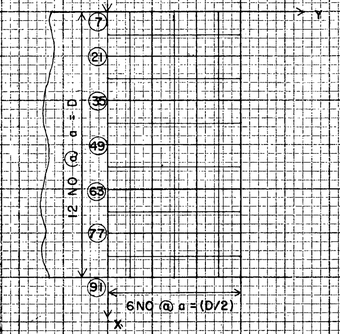

EXAMPLE 1

SEMI INFINITE PLATE, CONCENTRATED LOAD NORMAL TO FREE EDGE

NOTE — AT POINTS ON X-AXIS

$\sigma_y = 0$, $\tau_{xy} = 0$, $u = 0$

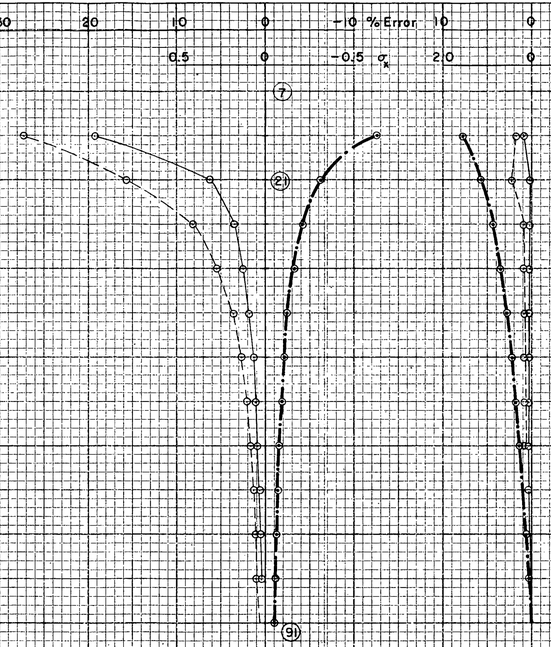

σ_x

$\mu = 0.4$

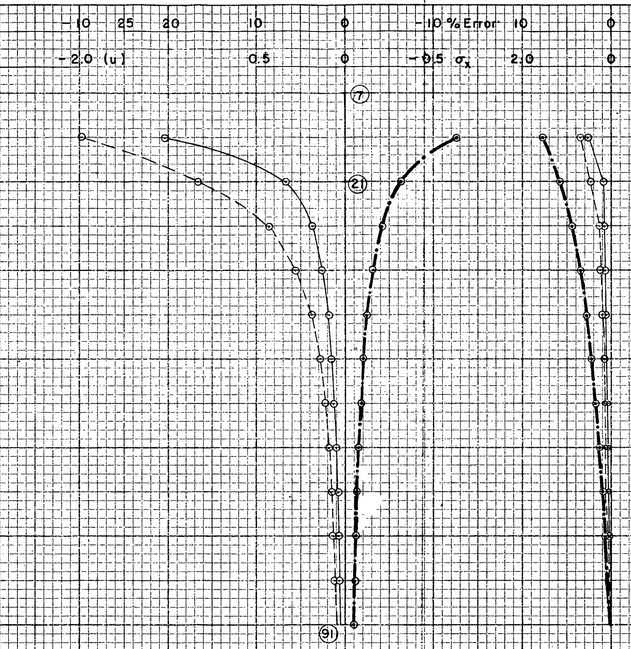

X-DISPLACEMENT (u)

σ_x

$\mu = 0.20$

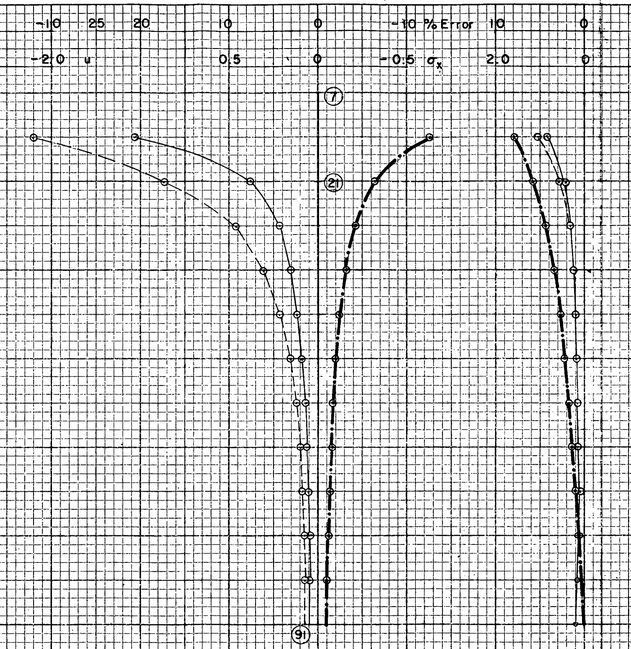

X-DISPLACEMENT (u)

$\mu = 0.0$

——— % ERROR WITH BAR MODEL

——— % ERROR WITH NO-BAR MODEL

—·—·— ELASTICITY SOLUTION

NOTE 1. DISPLACEMENTS TO BE MULTIPLIED BY (P/E)

2. STRESSES TO BE MULTIPLIED BY (P/a)

3. POSITIVE PERCENTAGE ERROR SIGNIFIES THAT FINITE ELEMENT RESULT NUMERICALLY LOWER THAN TRUE SOLUTION

PLATE - 1

EXAMPLE - 1

RESULTS AT NODAL POINTS ALONG X-AXIS FOR $\mu = 0.0, 0.2$ & 0.4

RESULTS ALONG SECTION B B

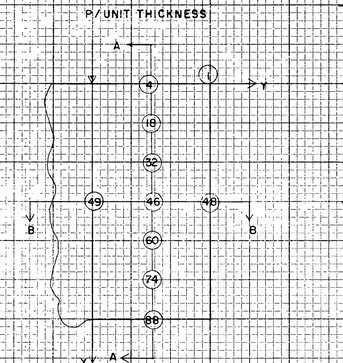

EXAMPLE $\mu = 1/3$

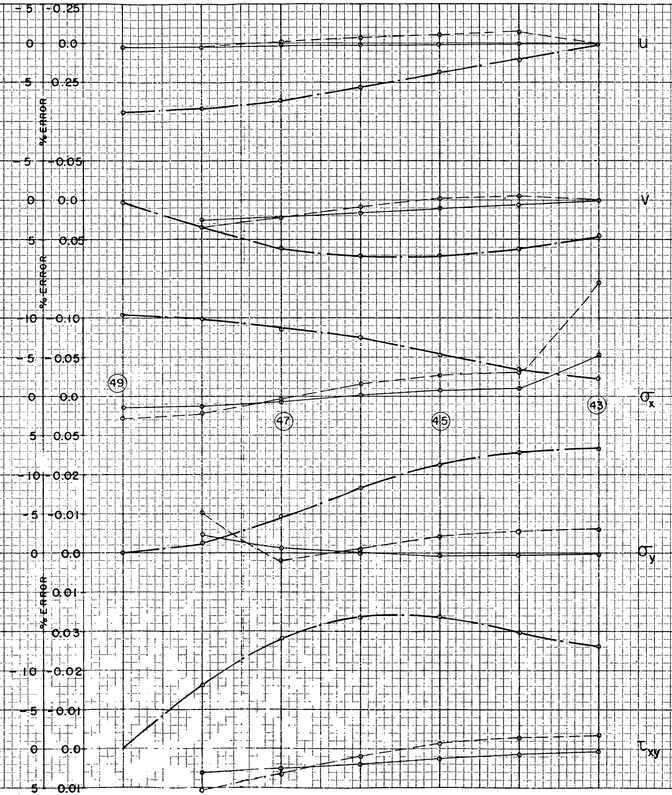

RESULTS ALONG SECTION A A

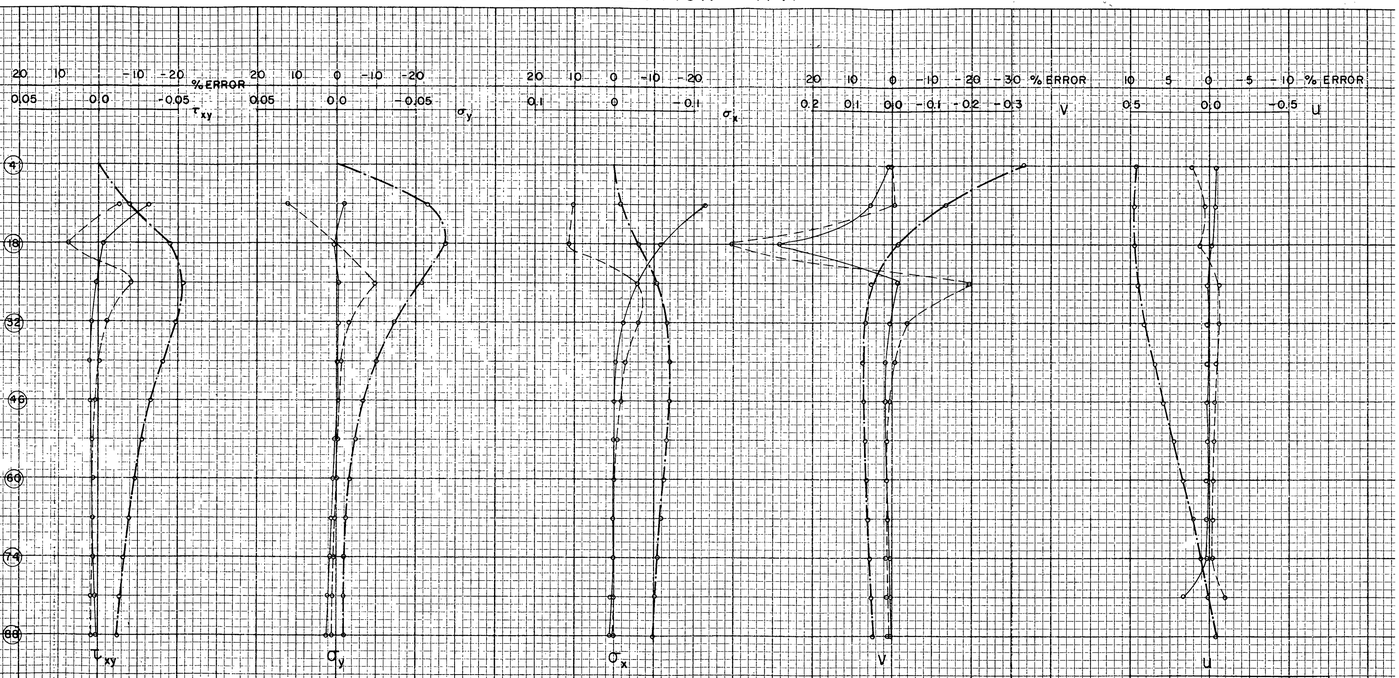

NOTE 1. FIGURES FOR u & v TO BE MULTIPLIED BY P/E
2. FIGURES FOR σ_x, σ_y, τ_{xy} TO BE MULTIPLIED BY (P/a)

——— % ERROR BY BAR MODEL
– – – – % ERROR BY NO-BAR MODEL
—— —— ELASTICITY SOLUTION

PLATE – 2

EXAMPLE – 1

$\mu = 1/3$

RESULTS ALONG SECTION BB

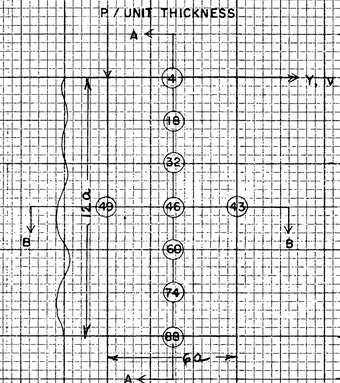

EXAMPLE – 1 $\mu = 0.0$

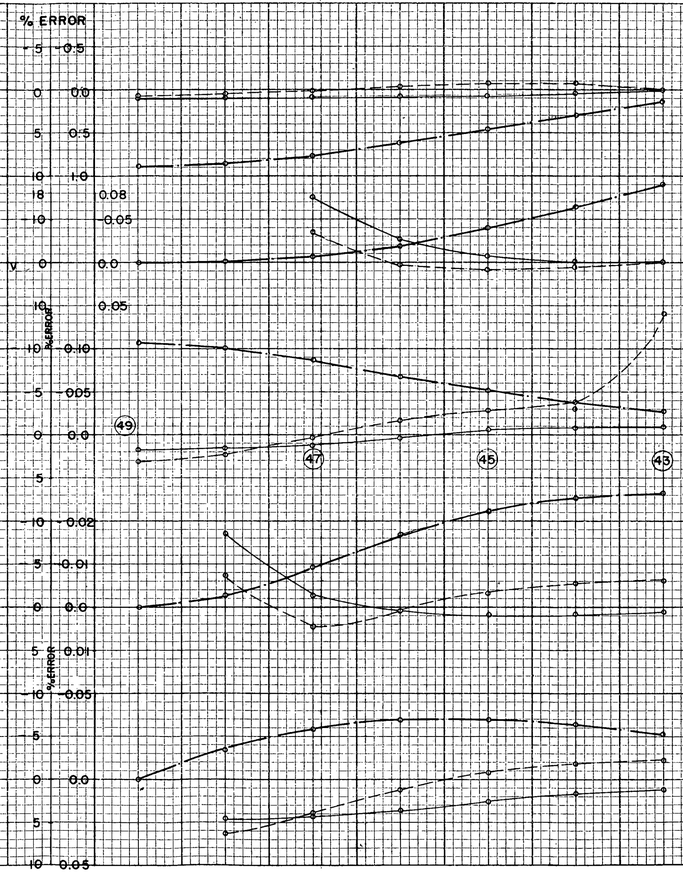

RESULTS ALONG SECTION AA

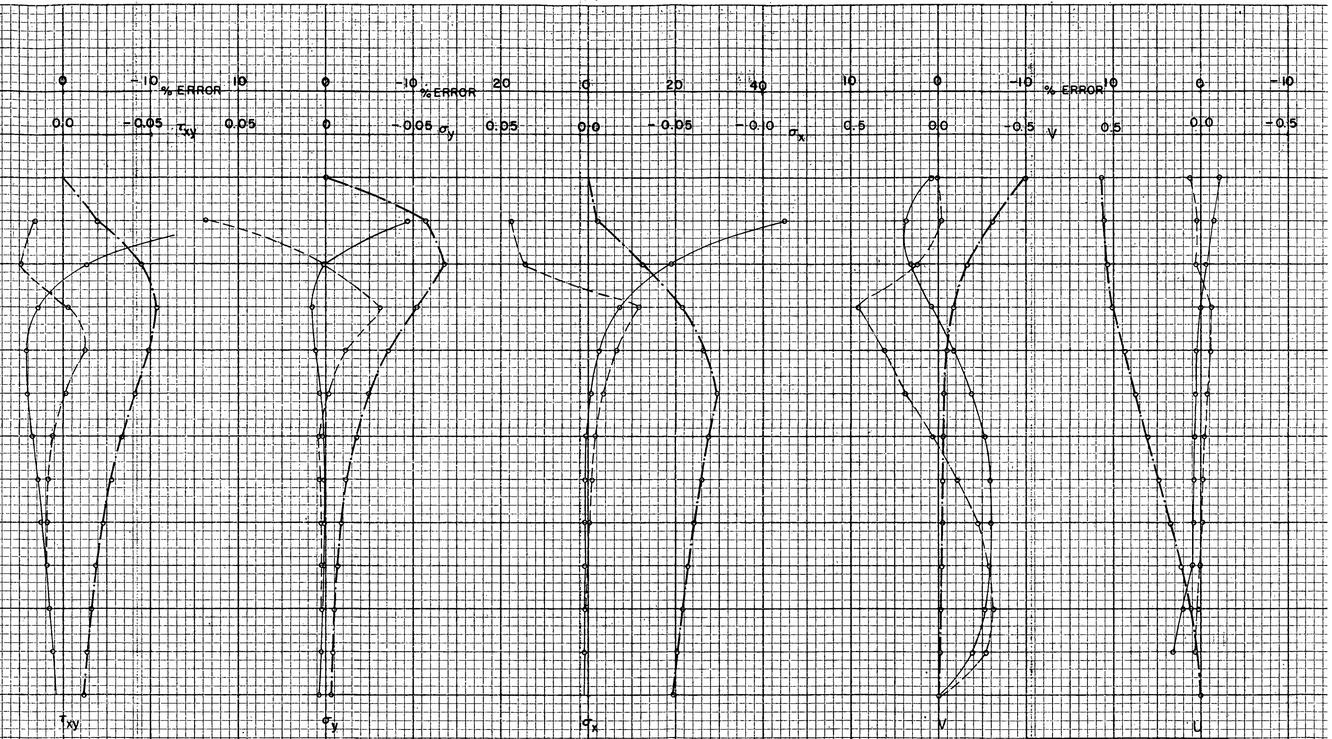

NOTE 1. FIGURES FOR U & V TO BE MULTIPLIED BY P/E
2. FIGURES FOR σ_x, σ_y & τ_{xy} TO BE MULTIPLIED BY (P/a)

——— % ERROR BY BAR MODEL
– – – % ERROR BY NO-BAR MODEL
—·— ELASTICITY SOLUTION

PLATE – 3
EXAMPLE – 1
$\mu = 0.0$

RESULTS AT NODAL POINTS ON X – AXIS

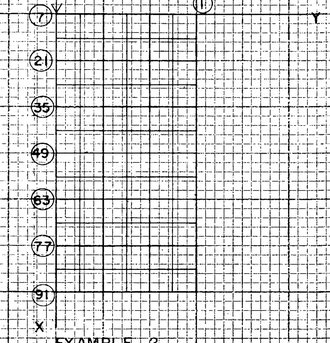

EXAMPLE 2

INFINITE PLATE WITH A CONC. FORCE ACTING IN ITS PLANE

NOTE AT POINTS ON X–AXIS
$\tau_x = 0$; $v = 0$

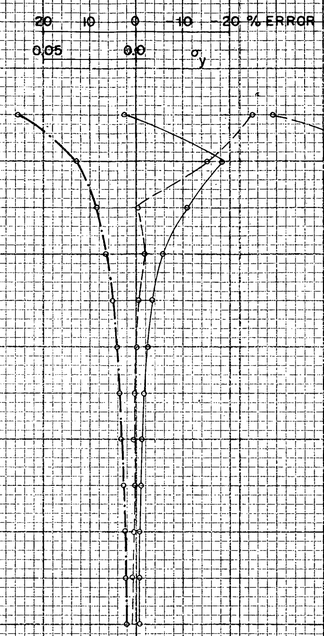

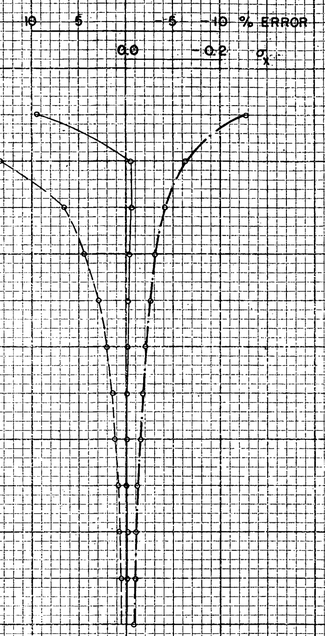

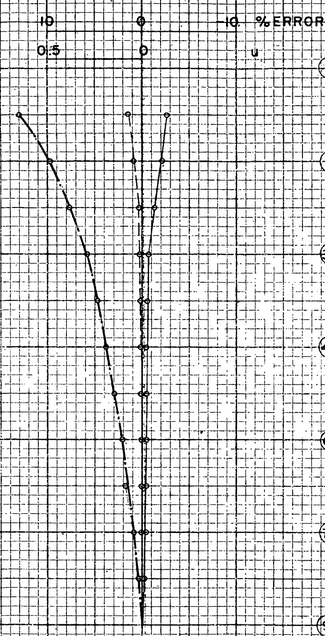

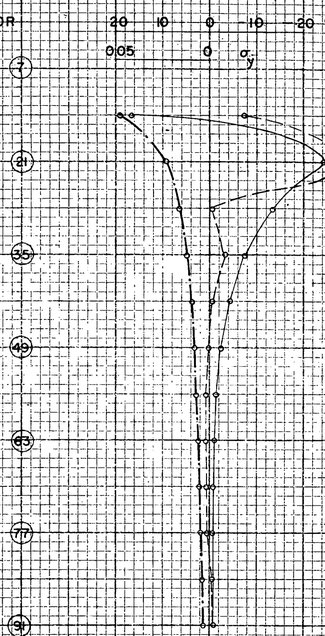

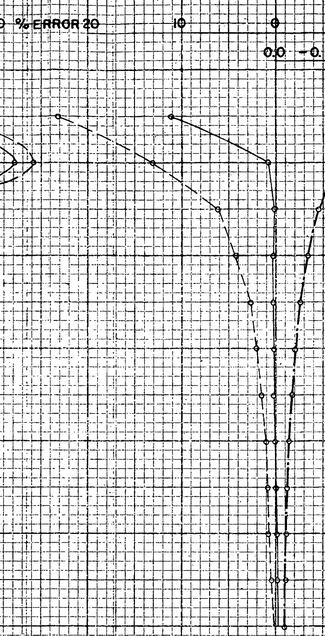

NOTE : 1. FIGURES FOR u & v TO BE MULTIPLIED BY (P/E)
2. FIGURES FOR σ_x & σ_y TO BE MULTIPLIED BY (P/a)

——— % ERROR WITH BAR MODEL
– – – – % ERROR WITH NO-BAR MODEL
—.—.— ELASTICITY SOLUTION

PLATE – 4
EXAMPLE 2
INFINITE PLATE WITH CONC. LOAD IN ITS PLANE. RESULTS ALONG X-AXIS; $\mu = 0.2$ & 0.4

RESULTS ALONG SECTION B B

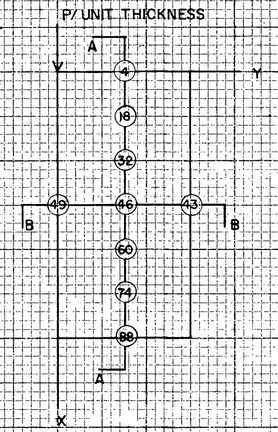

EXAMPLE – 2 , $\mu = 0.4$

NOTE
AT JOINT (4) (ON Y-AXIS) $\sigma_x = 0, \tau_{xy} = 0$
AT JOINT (49) (ON X-AXIS) $\tau_{xy} = 0$

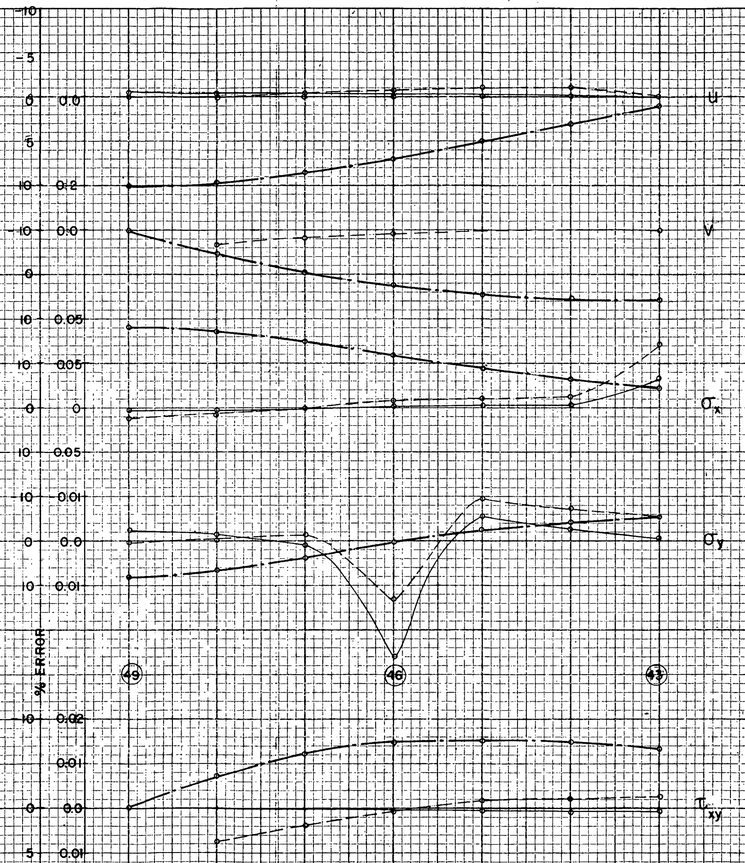

RESULTS ALONG SECTION AA

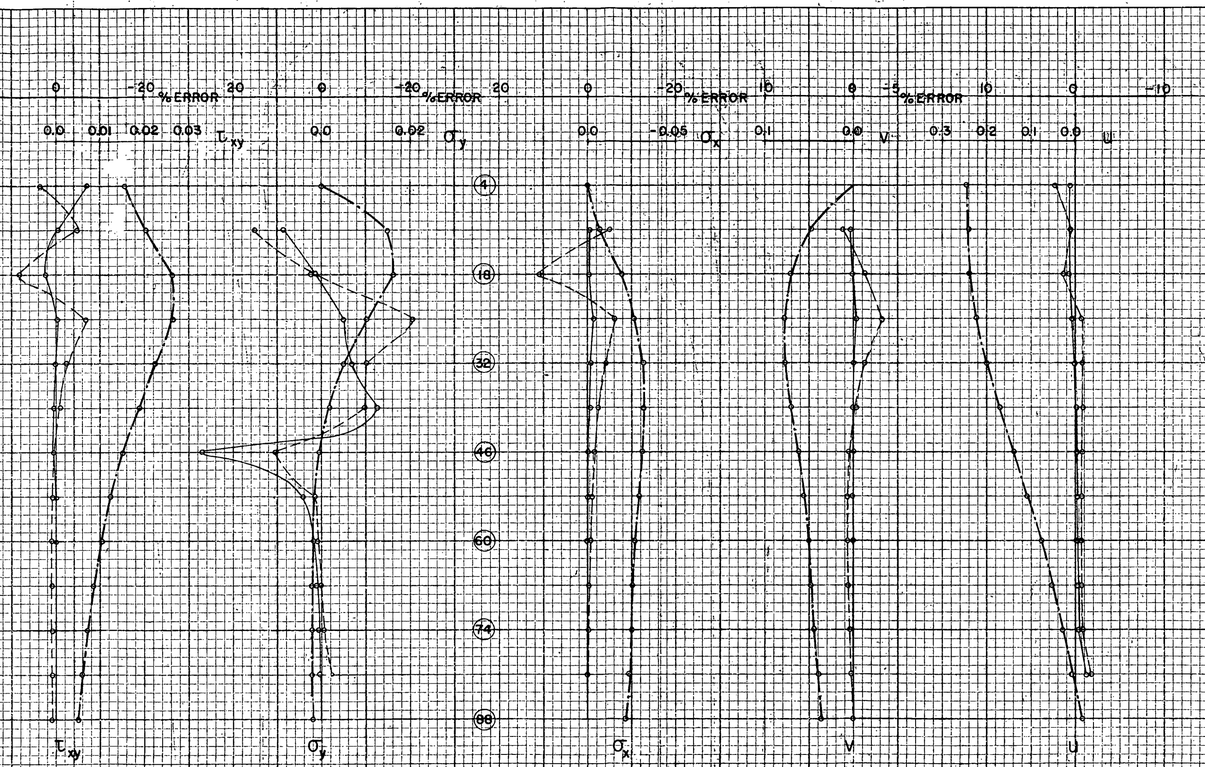

NOTE 1. FIGURES FOR U & V TO BE MULTIPLIED BY P/E
2. FIGURES FOR σ_x, σ_y & τ_{xy} TO BE MULTIPLIED BY (P/a)

PLATE – 5
EXAMPLE – 2
$\mu = 0.4$

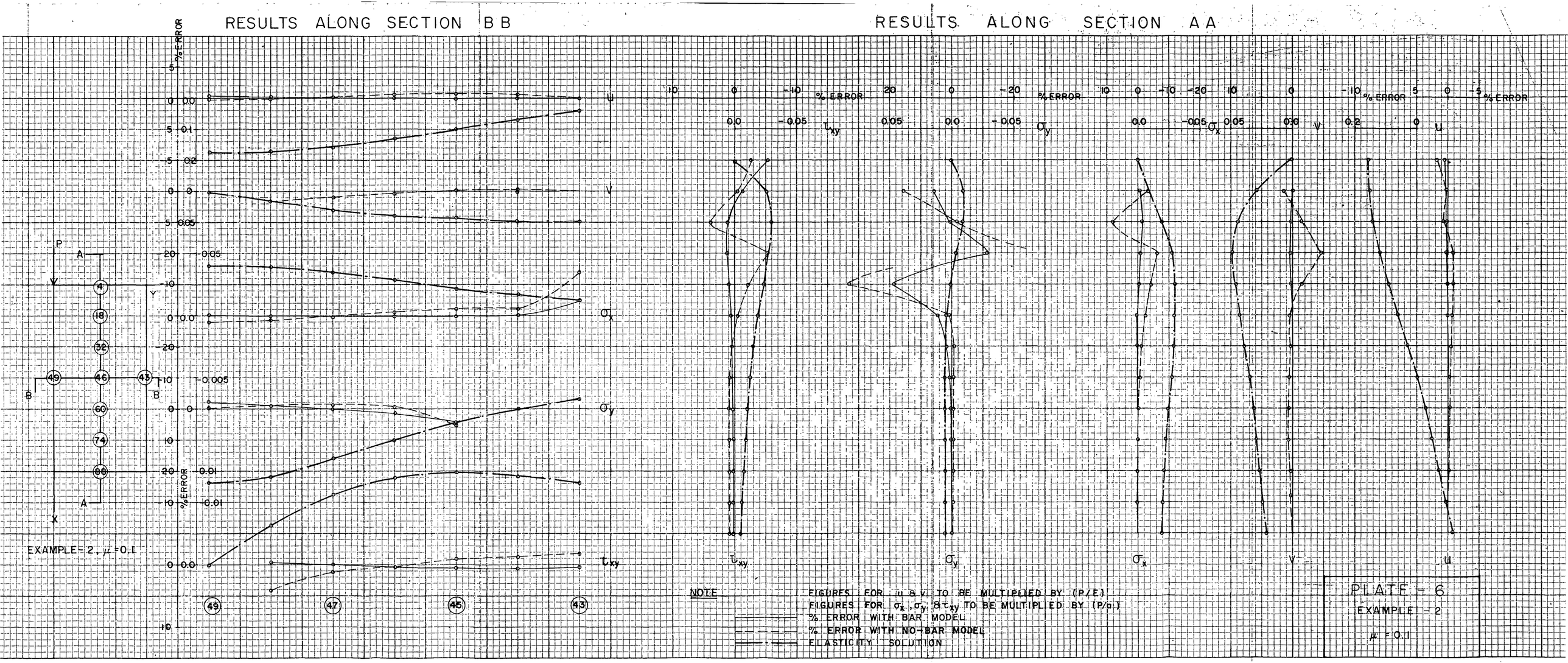
RESULTS ALONG SECTION B B
RESULTS ALONG SECTION A A
% ERROR
u
v
σx
σy
τxy
P
A
B
X
Y
EXAMPLE- 2, μ =0.1
NOTE
FIGURES FOR u & v TO BE MULTIPLIED BY (P/E)
FIGURES FOR σx, σy & τxy TO BE MULTIPLIED BY (P/a)
% ERROR WITH BAR MODEL
% ERROR WITH NO-BAR MODEL
ELASTICITY SOLUTION
PLATE - 6
EXAMPLE - 2
μ = 0.1

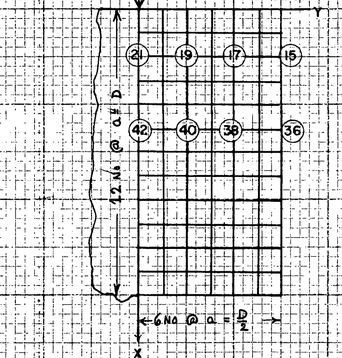

EXAMPLE - I

NOTE

1. ——— % ERROR BY BAR MODEL
   - - - - % ERROR BY NO-BAR MODEL
   ——— ELASTICITY SOLUTION
2. σ_x, σ_y & τ_{xy} ARE INDEPENDENT OF μ
3. u & v AT ANY POINT ARE LINEAR FUNCTIONS OF μ
4. FIGURES FOR u & v TO BE MULTIPLIED BY (P/E)

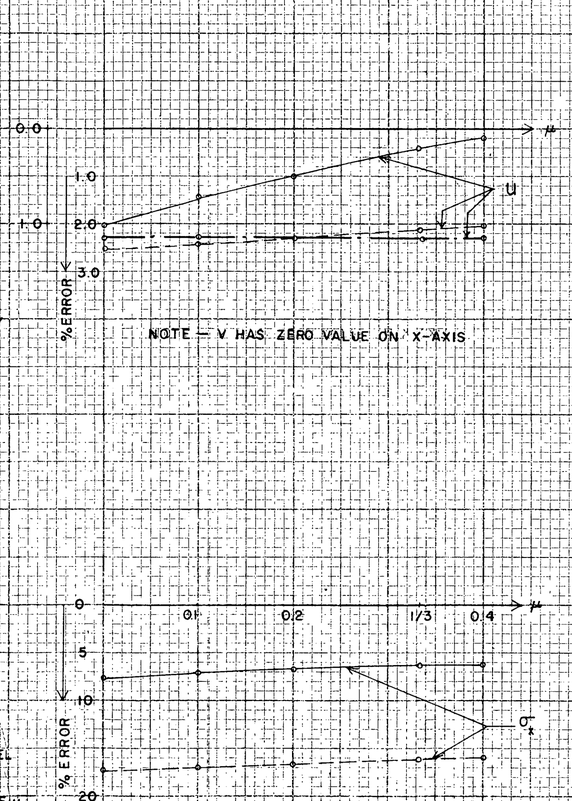

NOTE — V HAS ZERO VALUE ON X-AXIS

JOINT (21)

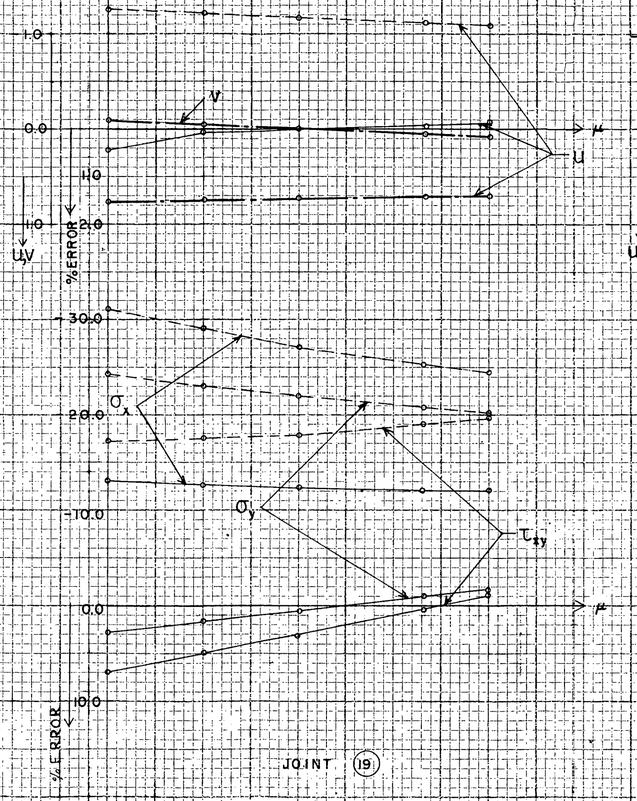

JOINT (19)

NOTE VALUES OF V AT (19) ARE VERY SMALL
% ERROR BY F.E. METHOD IS LARGE
AND NOT SHOWN IN THE FIGURE

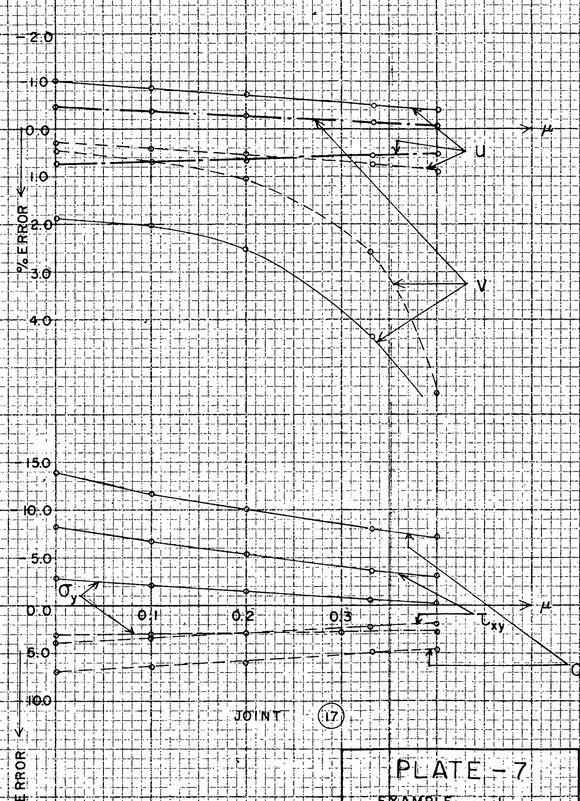

JOINT (17)

PLATE - 7

EXAMPLE — I
μ vs % ERROR
FOR JOINTS (17) (19) (21)

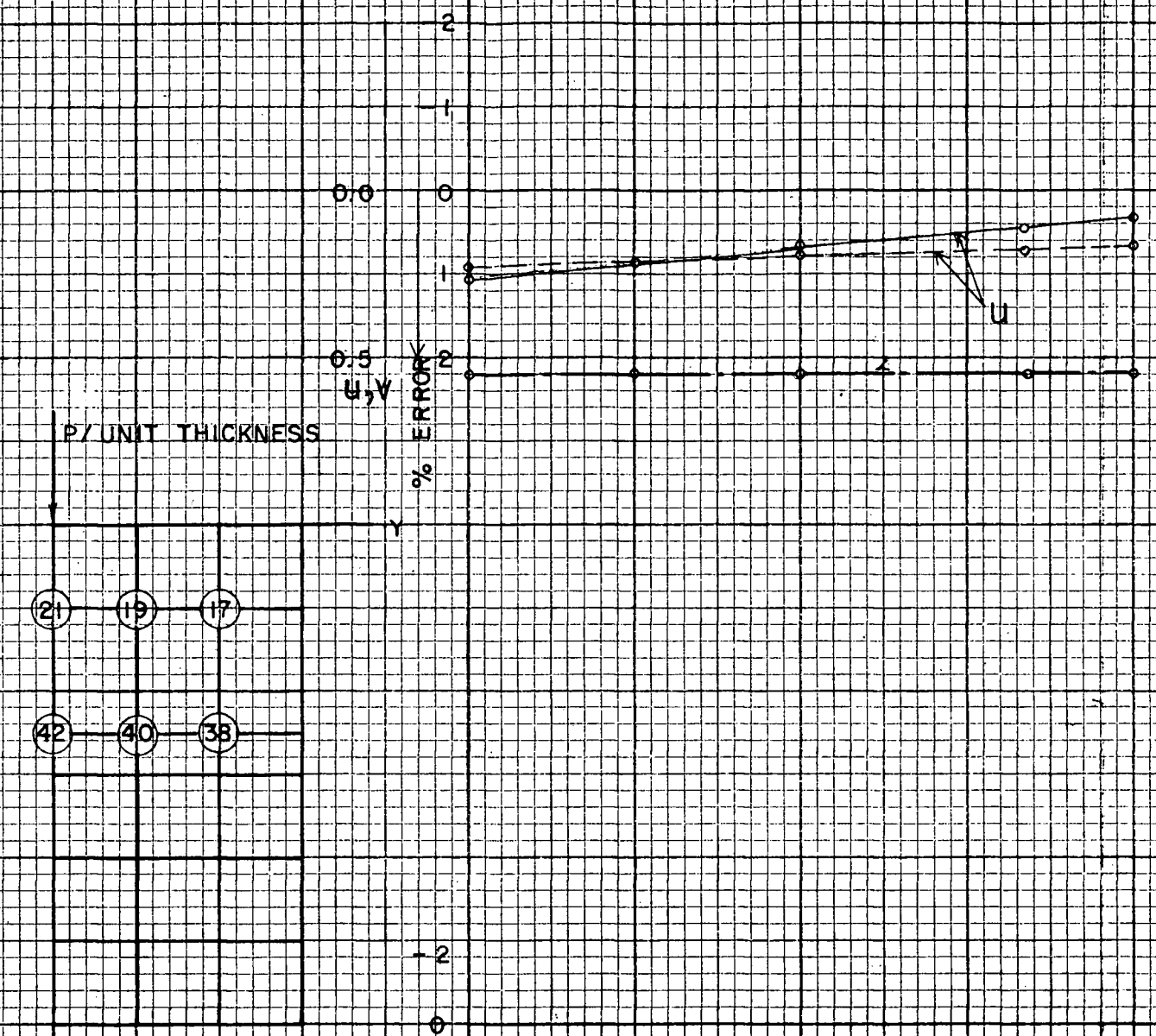

EXAMPLE – 1

JOINT (42)

NOTE – σ_y, τ_{xy} AND V HAVE ZERO VALUES AT (42)

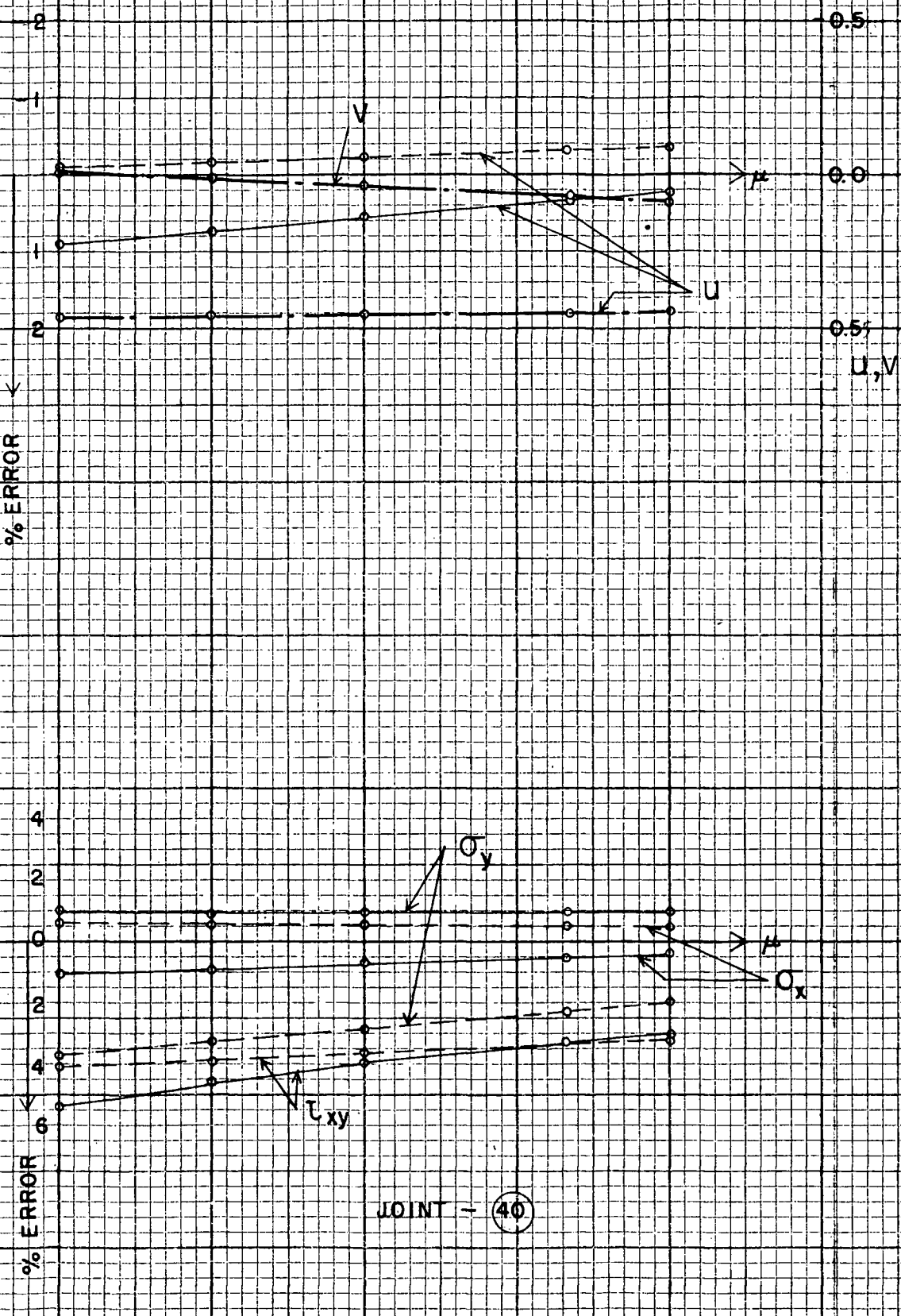

JOINT – (40)

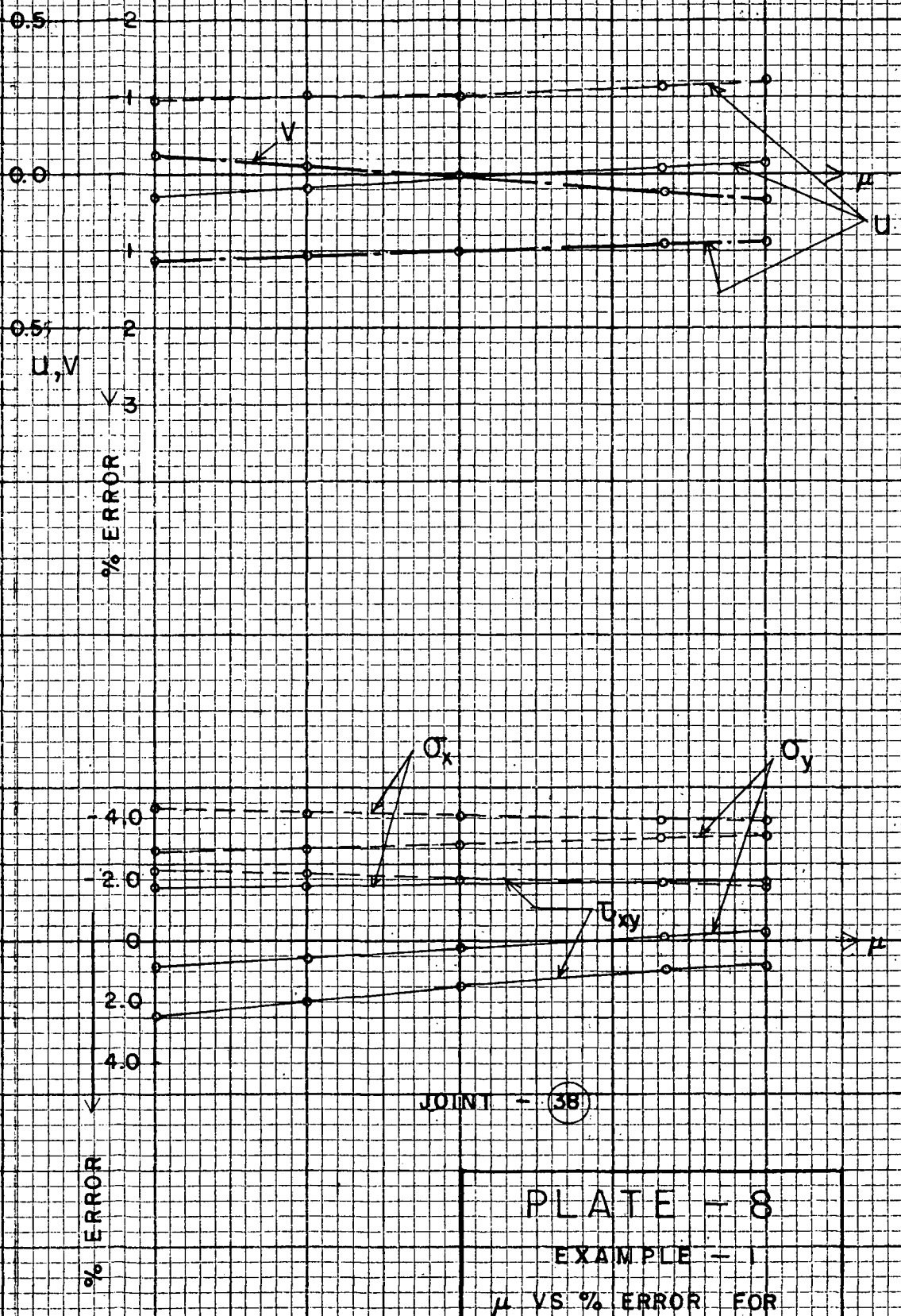

JOINT – (38)

PLATE – 8

EXAMPLE – 1

μ VS % ERROR FOR JOINTS (38), (40) AND (42)

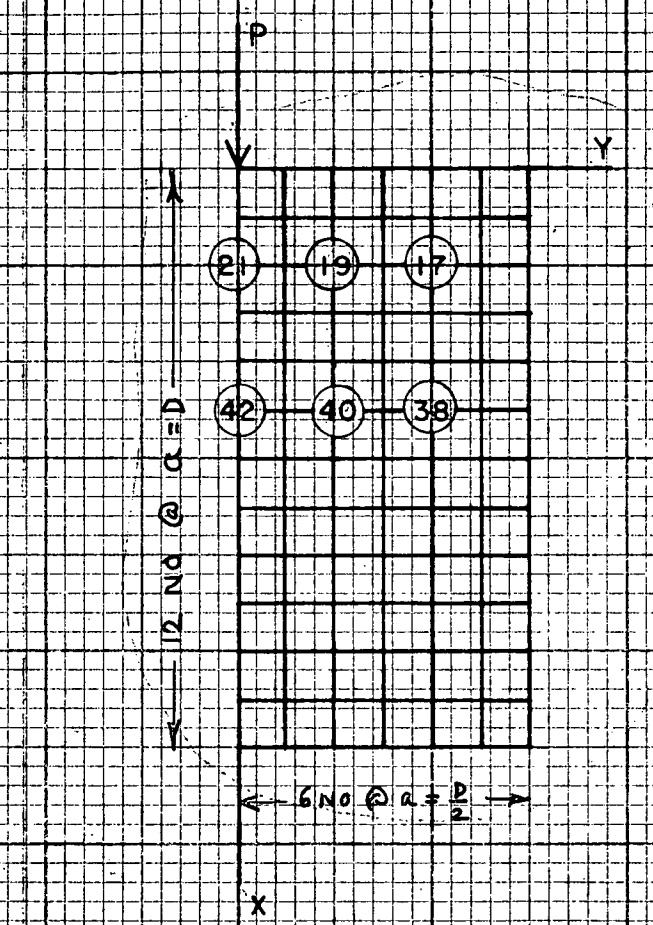

EXAMPLE – 2

NOTE
AT JOINT (21) τ_{xy} & V ARE ZERO

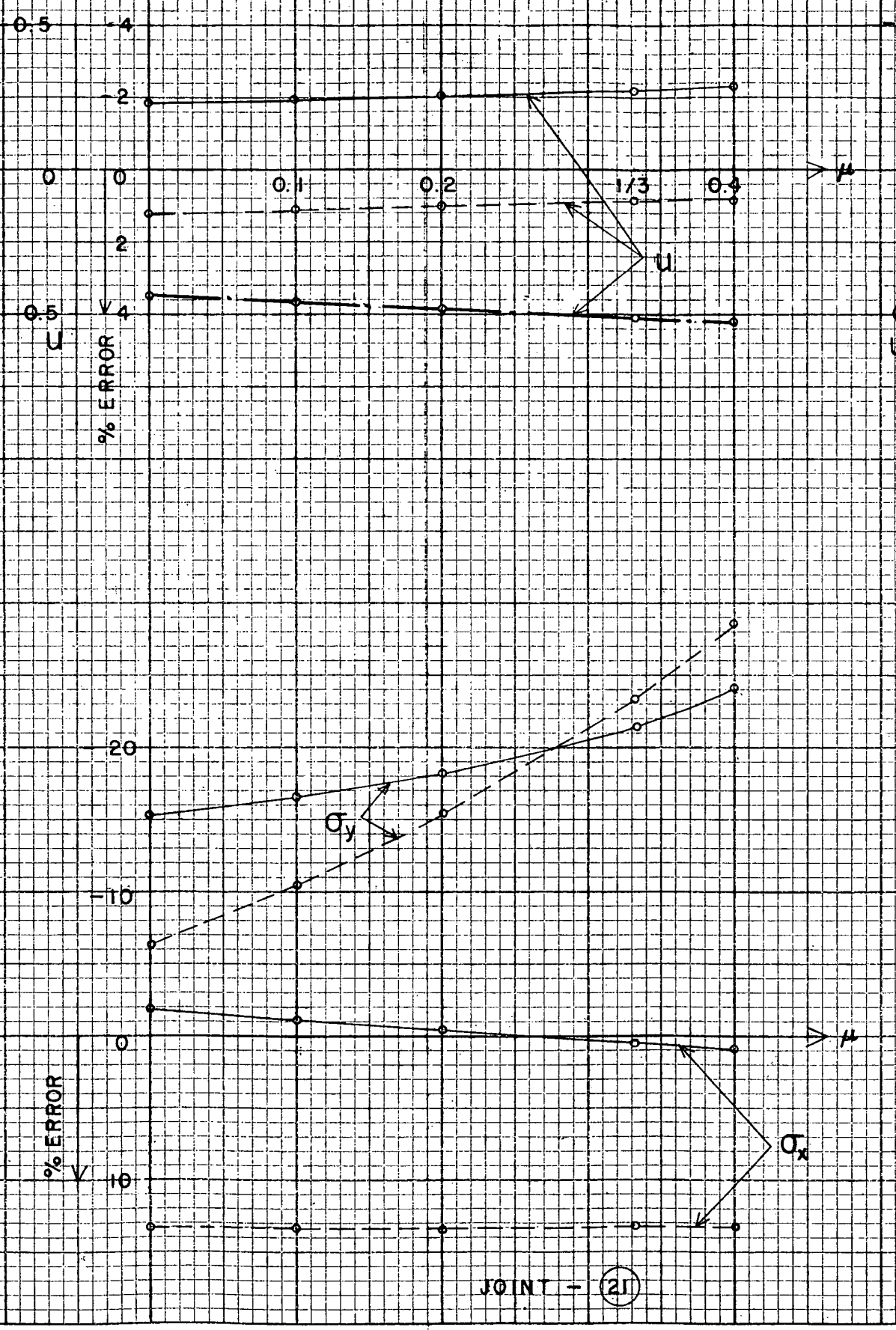

JOINT – (21)

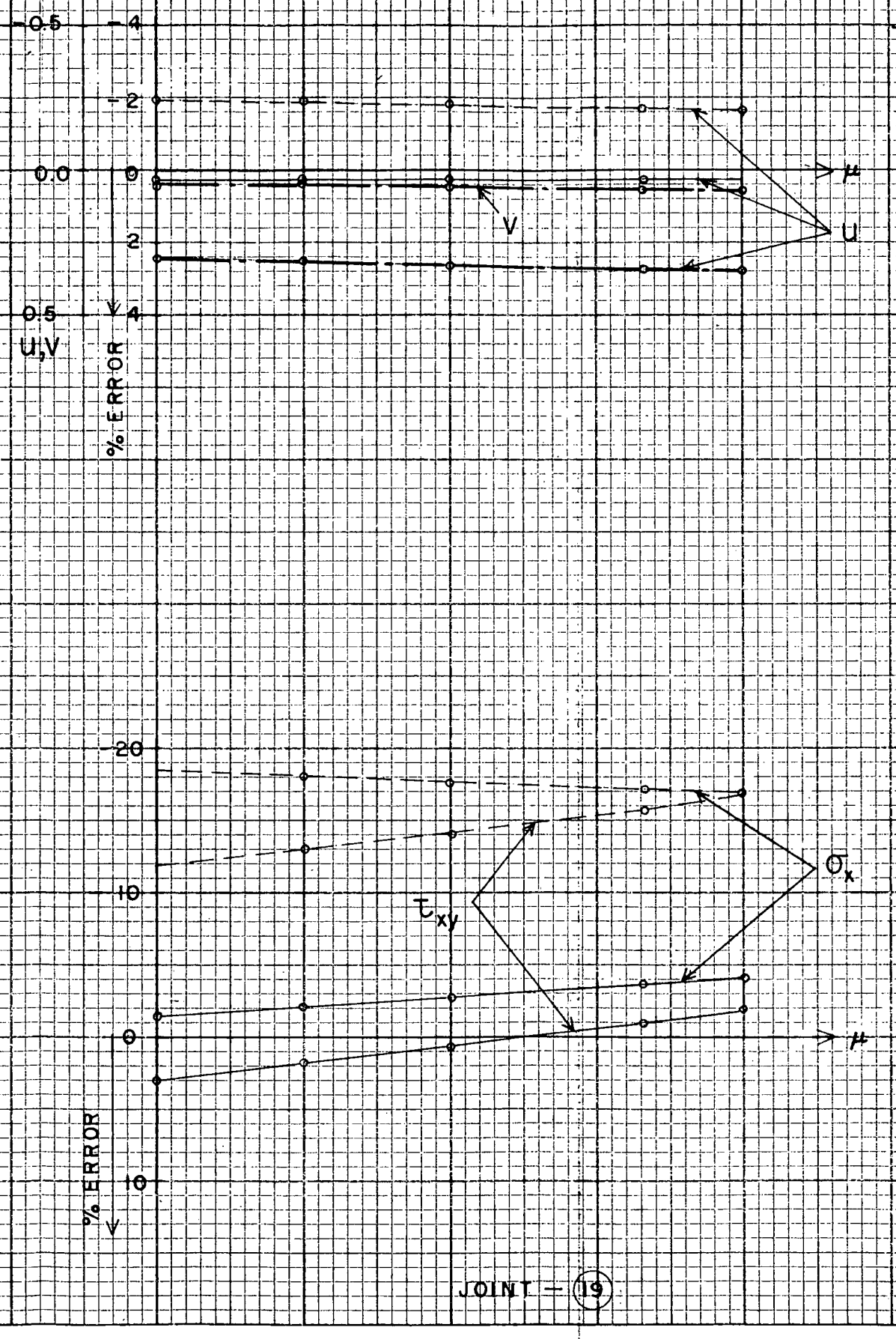

JOINT – (19)

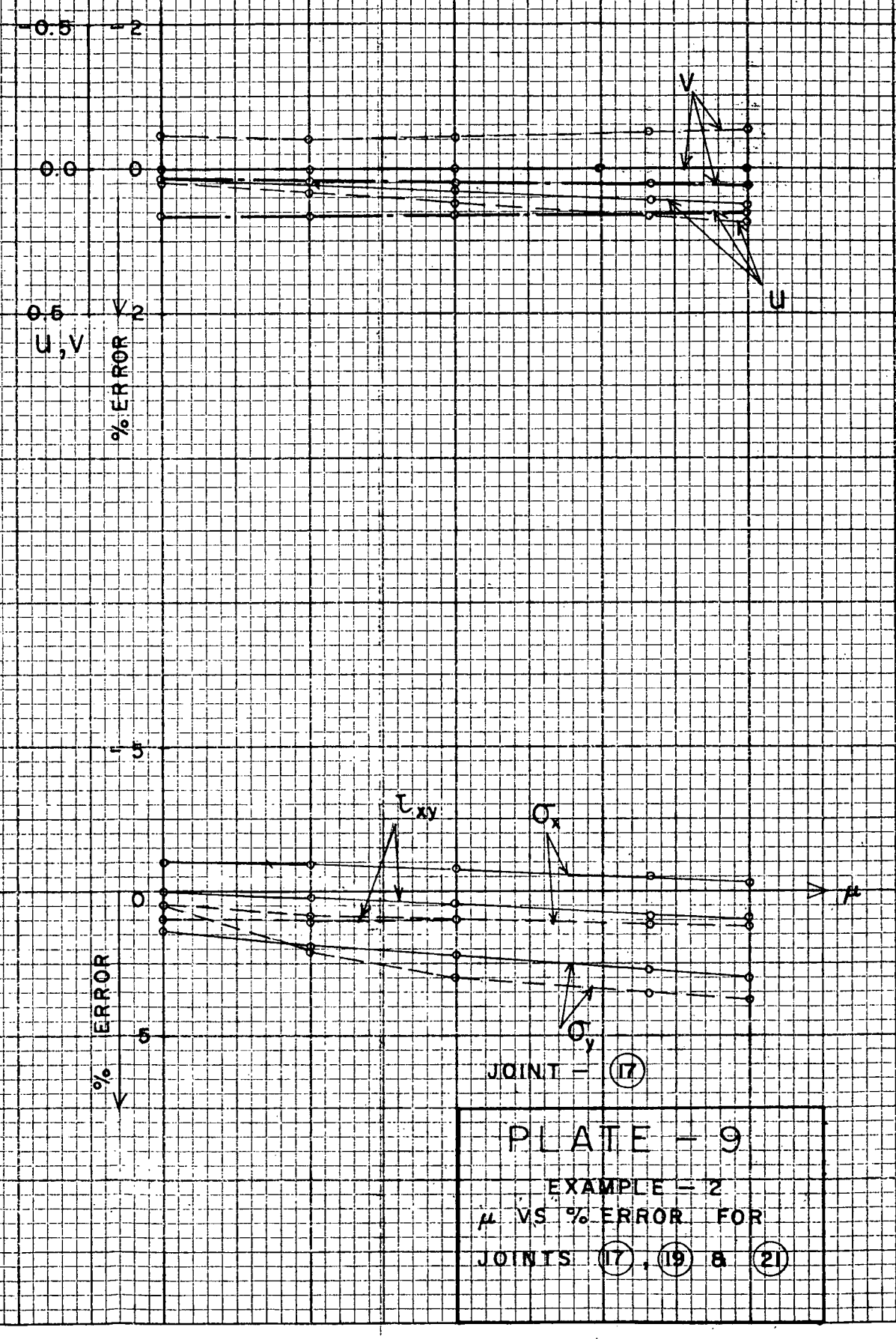

JOINT – (17)

PLATE – 9

EXAMPLE – 2

μ VS % ERROR FOR JOINTS (17), (19) & (21)

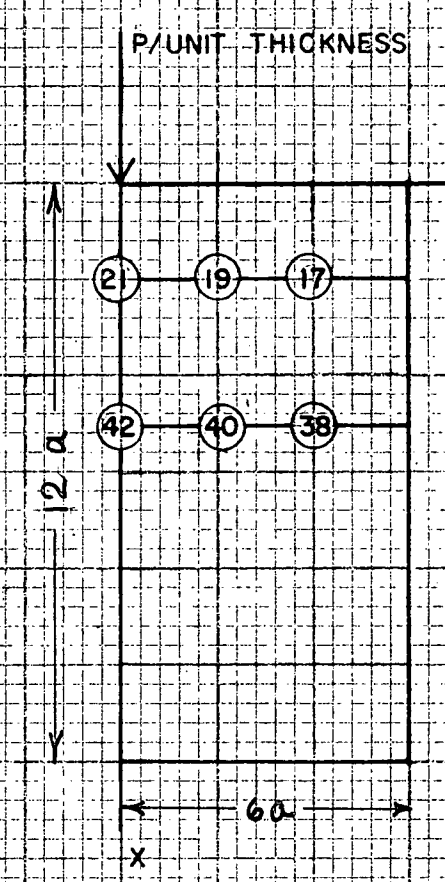

EXAMPLE – 2

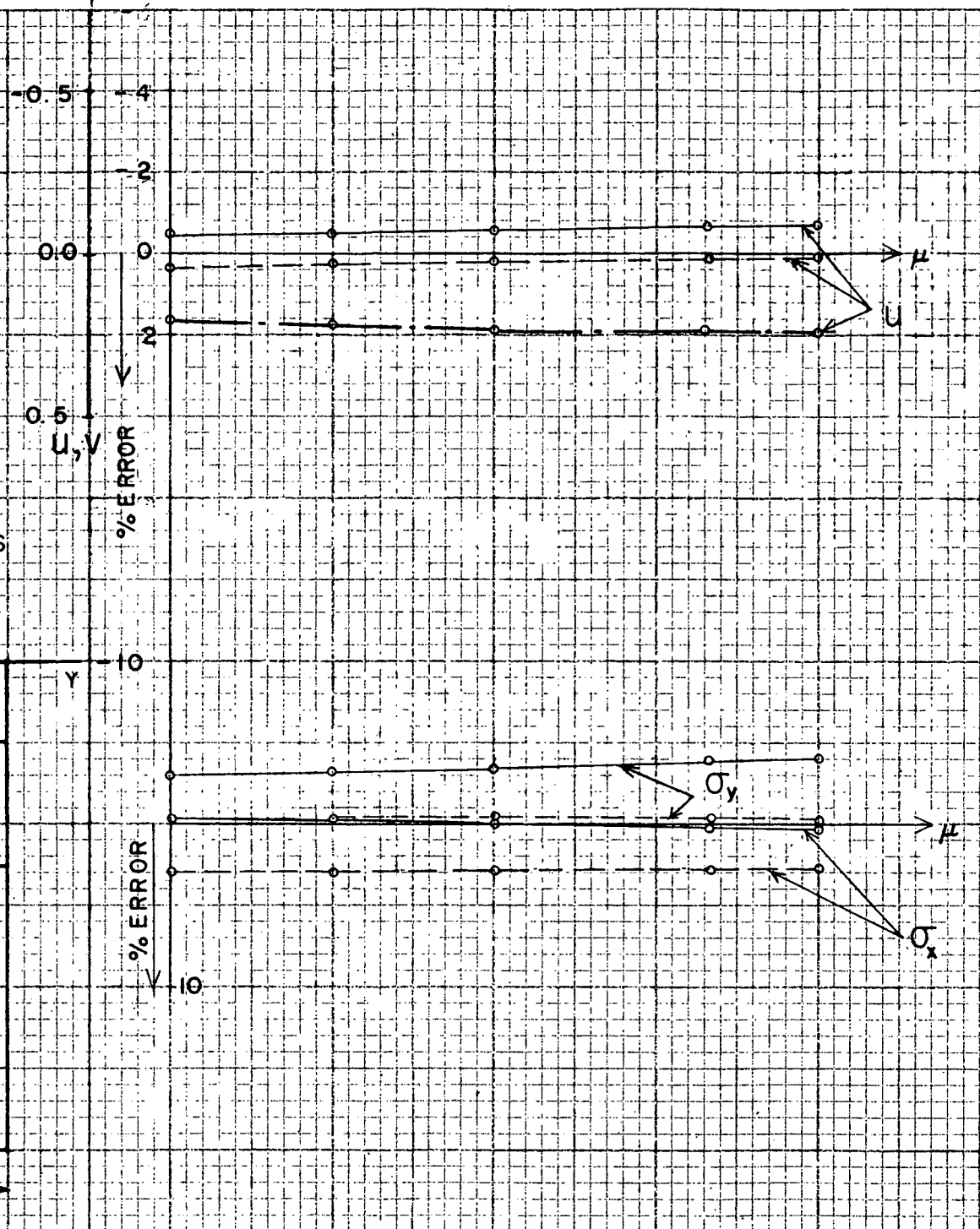

JOINT – (42)

NOTE AT JOINT (42) τ_{xy} & V ARE ZERO

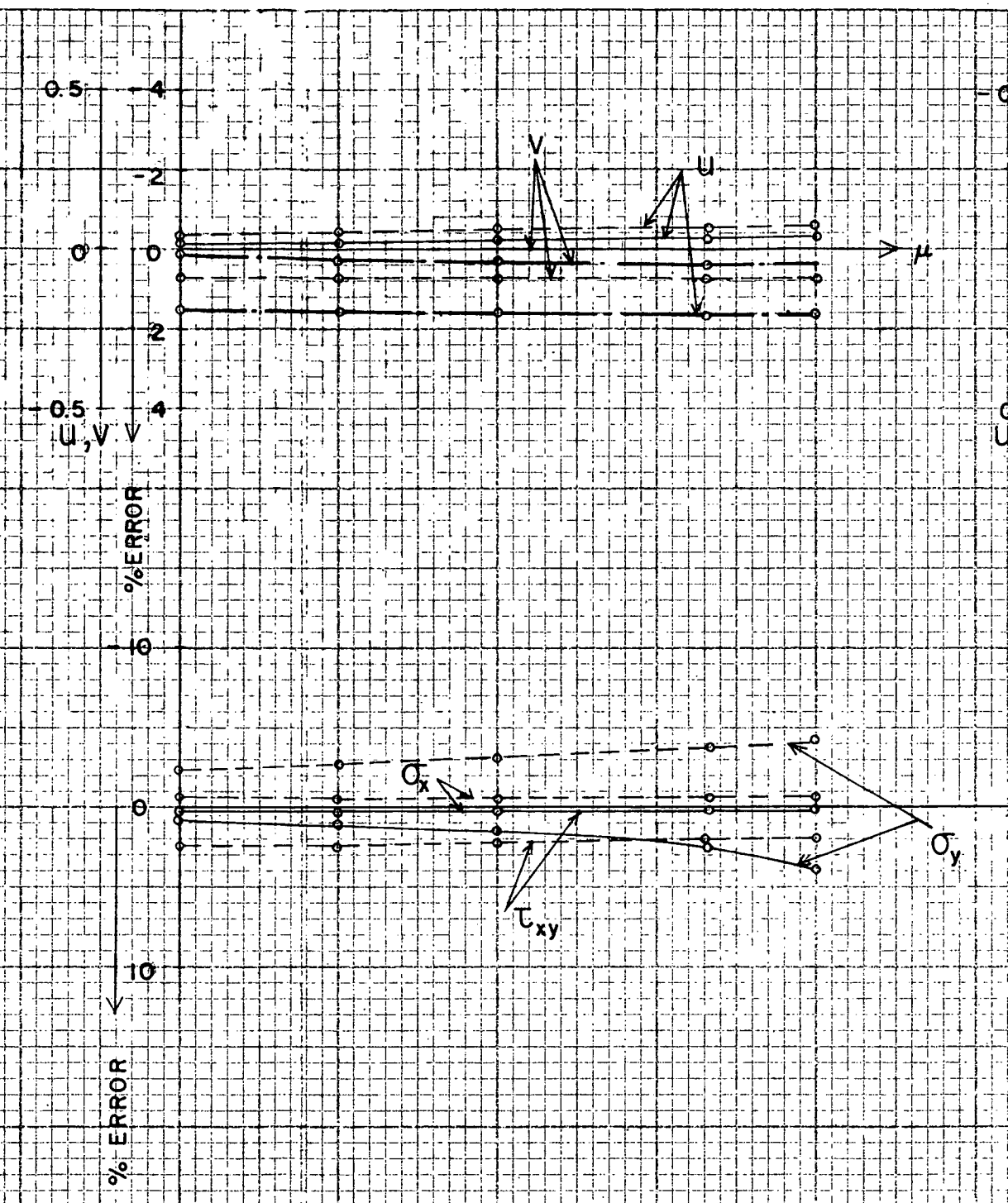

JOINT – (40)

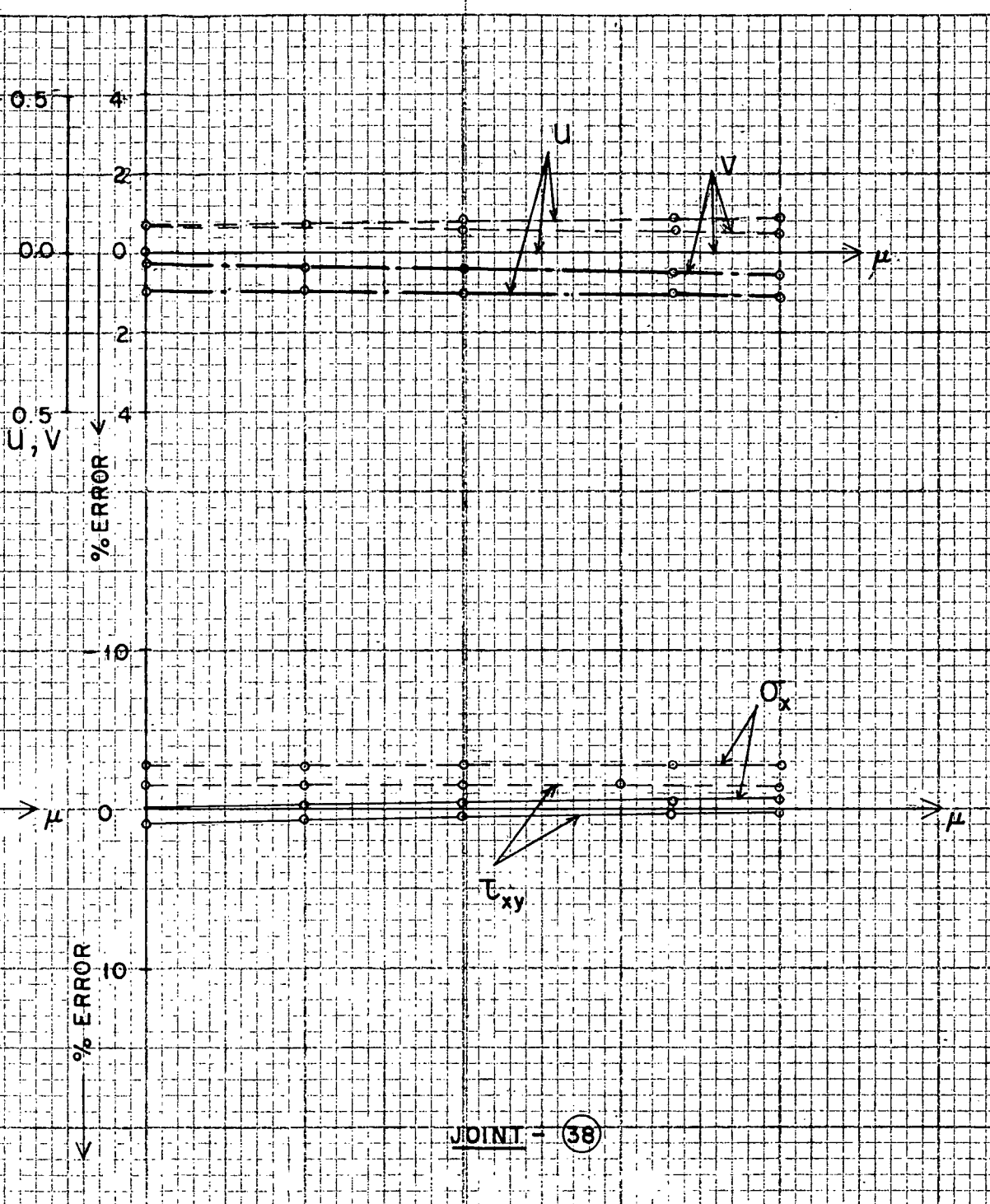

JOINT – (38)

VALUES OF σ_y ARE VERY SMALL WITH A LARGE % ERROR BY F.E. METHOD AND NOT SHOWN IN THE FIGURE

PLATE – 10

EXAMPLE – 2

μ VS % ERROR FOR JOINTS (38), (40) AND (42)

RESULTS ALONG BB

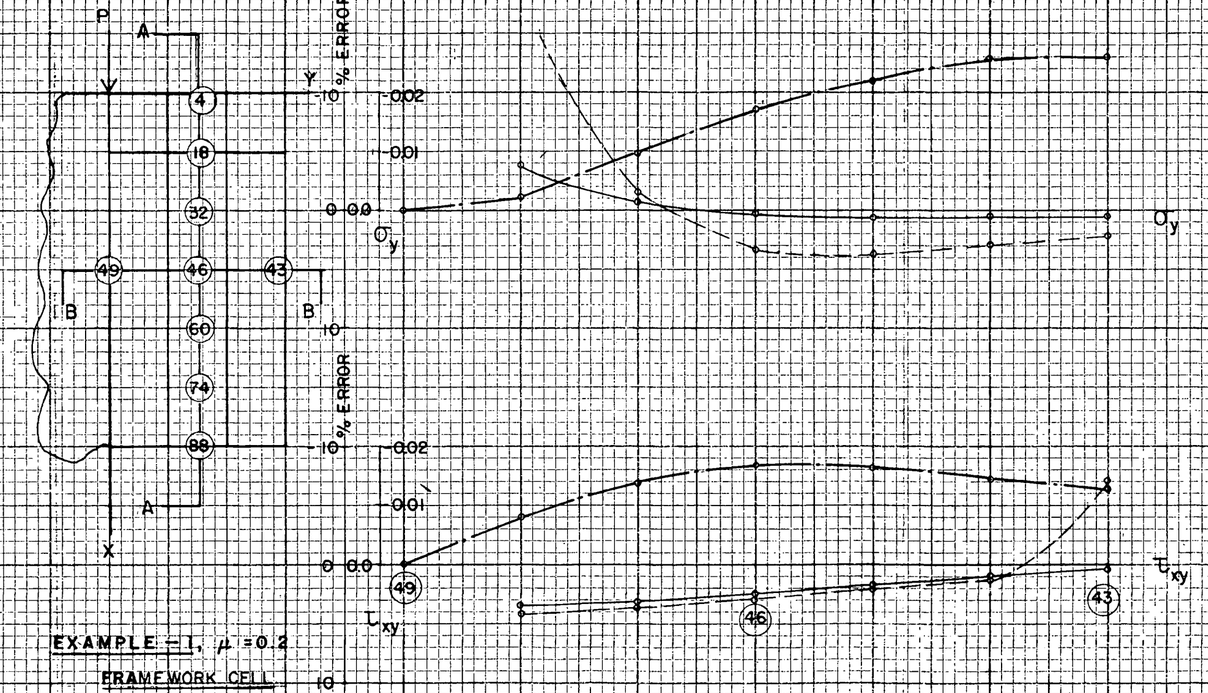

EXAMPLE – I, $\mu = 0.2$

FRAMEWORK CELL

NOTE

——— % ERROR IN STRESSES FROM NODAL CONCENTRATIONS

– – – – % ERROR IN STRESSES FROM JOINT DISPLACEMENTS

—·—·— ELASTICITY SOLUTION

FIGURES FOR STRESSES TO BE MULTIPLIED BY (P/a)

RESULTS ALONG AA

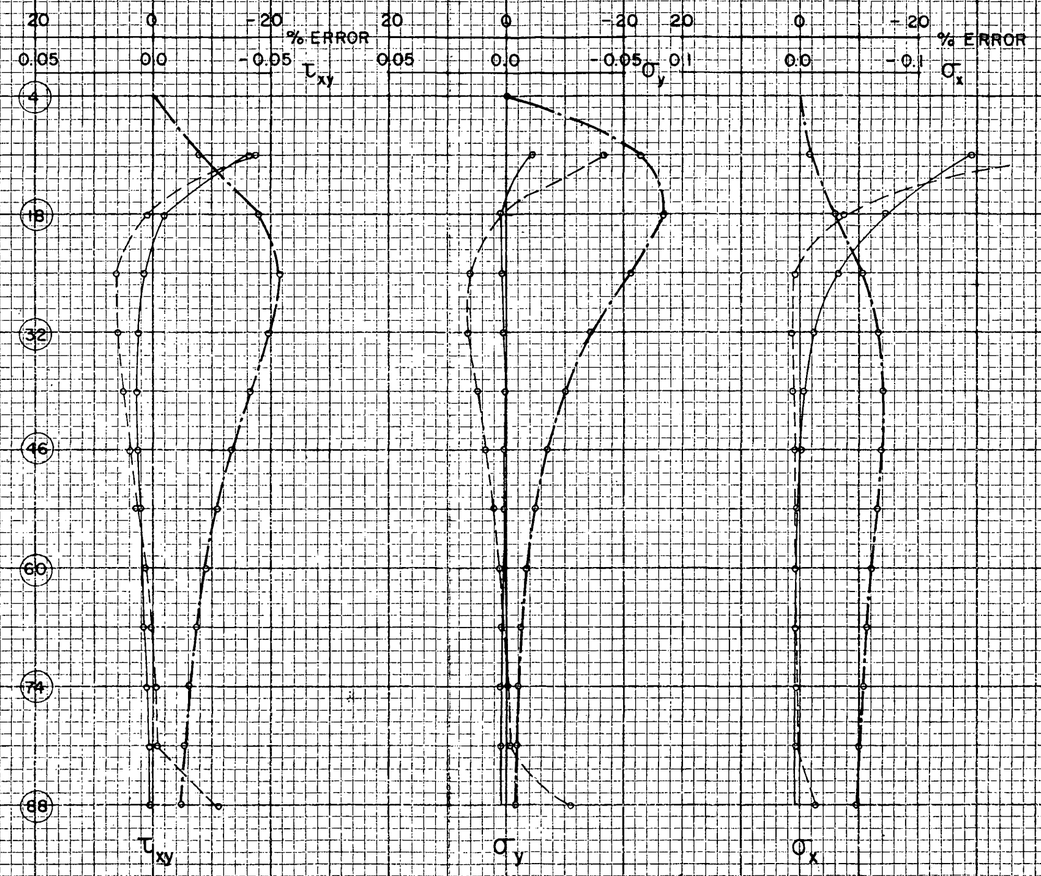

PLATE – II

EXAMPLE I

% ERROR OF STRESSES BY TWO METHODS ALONG SECTION AA & BB

$\mu = 0.2$

RESULTS ALONG SECTION B B

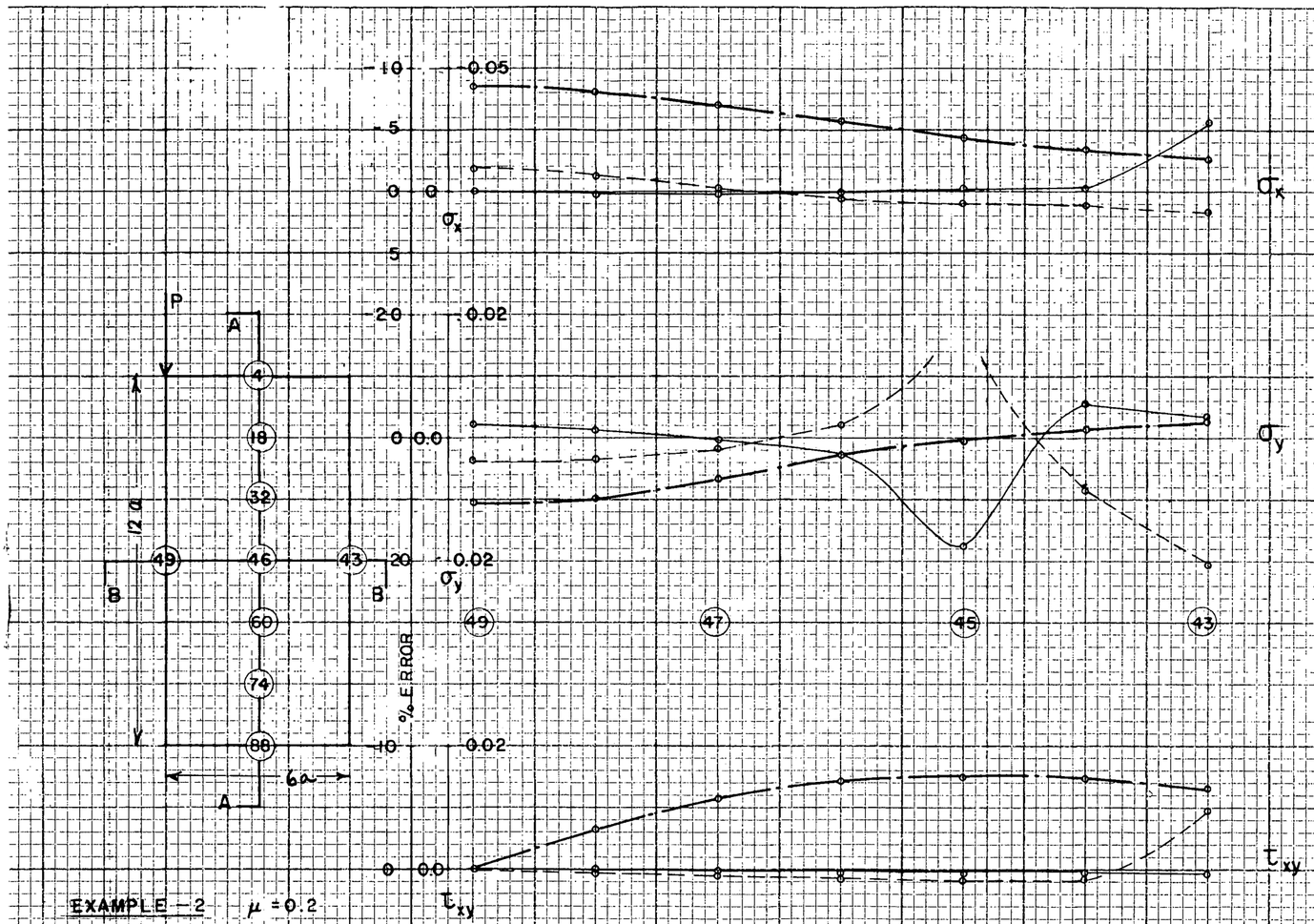

EXAMPLE – 2 $\mu = 0.2$

(FRAMEWORK CELL)

NOTES

——— % ERROR IN STRESSES, FROM NODAL CONCENTRATIONS

– – – – % ERROR IN STRESSES, FROM JOINT DISPLACEMENTS

——·—— ELASTICITY SOLUTION

FIGURES FOR STRESSES TO BE MULTIPLIED BY (P/a)

RESULTS ALONG SECTION A A

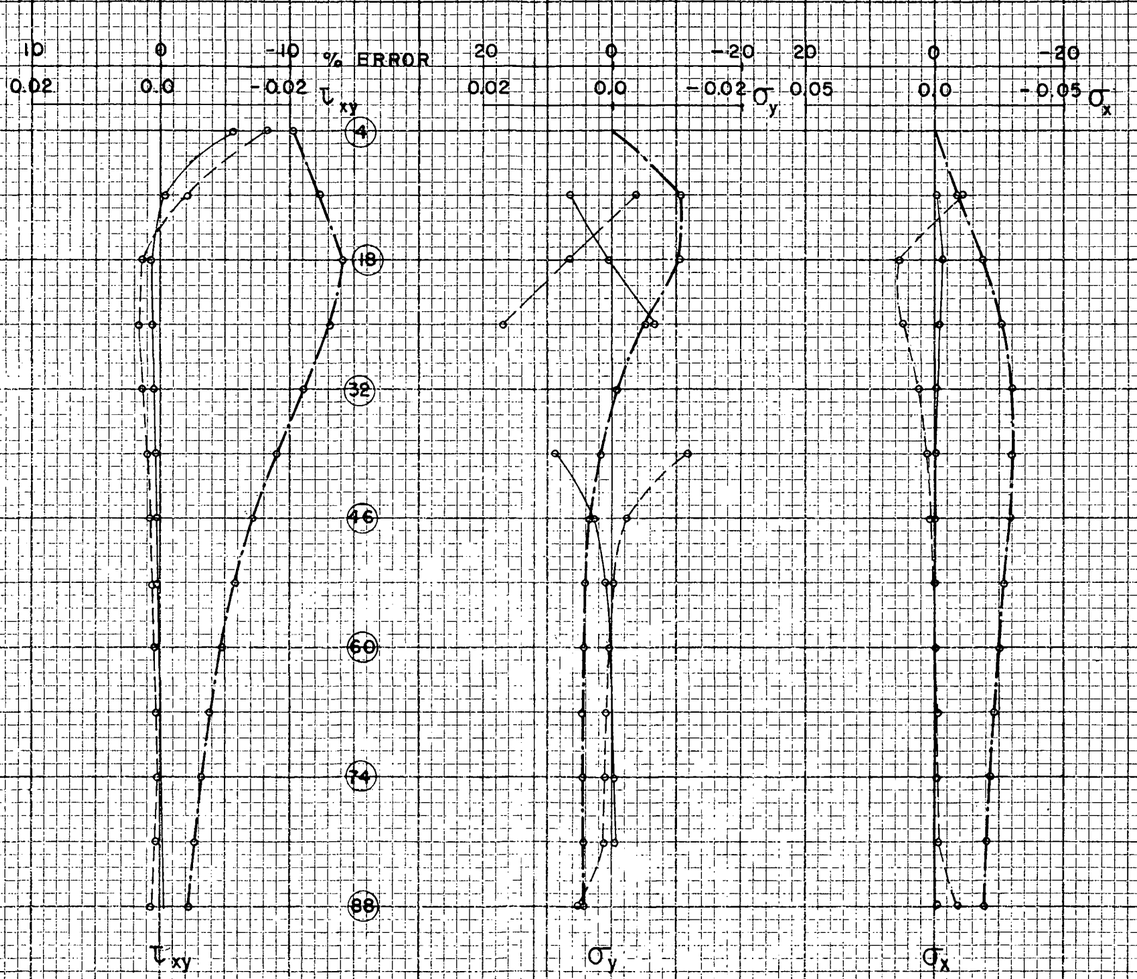

PLATE – 12

EXAMPLE – 2

% ERROR OF STRESSES ALONG AA & BB BY TWO METHODS. $\mu = 0.2$

RESULTS ALONG SECTION BB

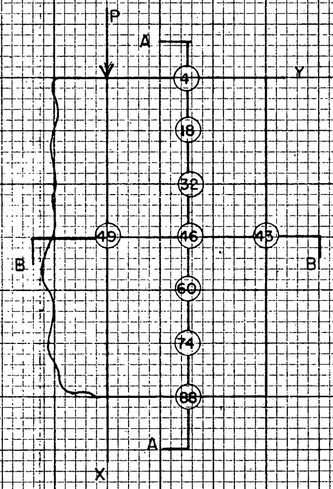

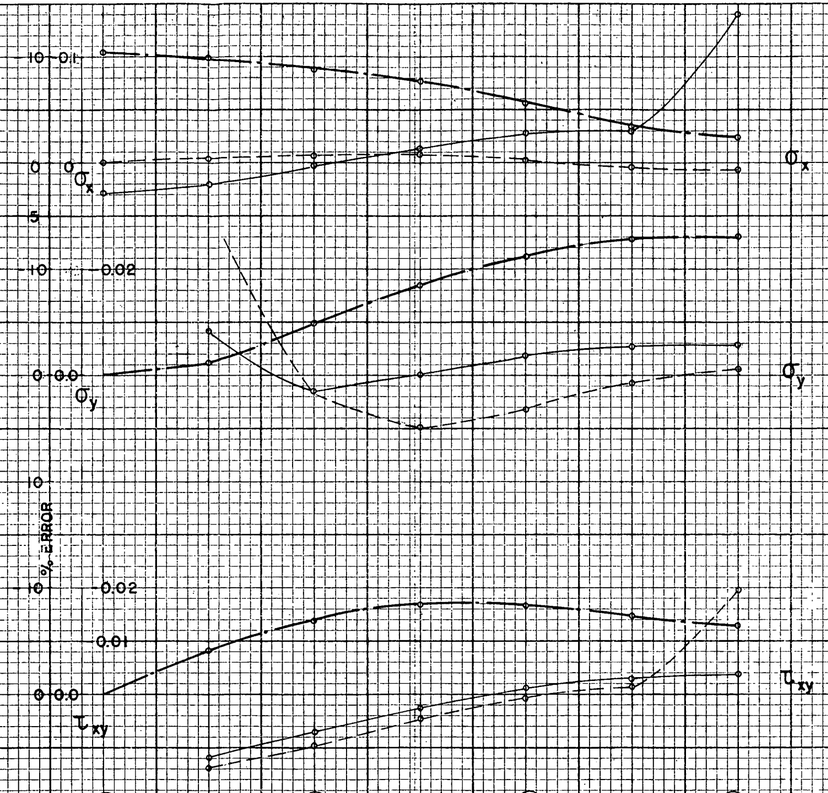

EXAMPLE 1, $\mu = 0.2$

NO-BAR MODEL

NOTE-1 ——— % ERROR IN STRESSES FROM NODAL CONCENTRATIONS

– – – – % ERROR IN STRESSES FROM JOINT DISPLACEMENTS

—·—·— ELASTICITY SOLUTION

NOTE-2 STRESSES TO BE MULTIPLIED BY (P/a)

RESULTS ALONG SECTION AA

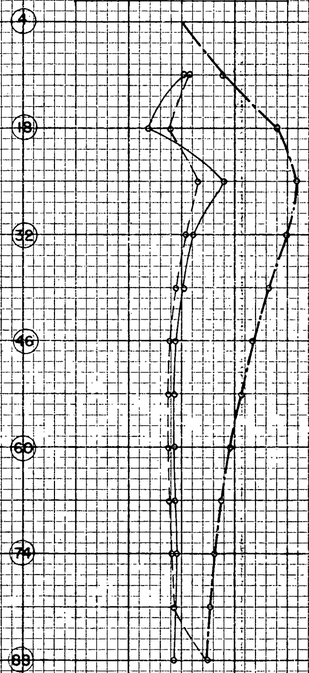

PLATE - 13

EXAMPLE - 1

NOBAR MODEL - % ERROR OF STRESSES ALONG AA AND BB FOR $\mu = 0.2$

RESULTS ALONG SECTION B B

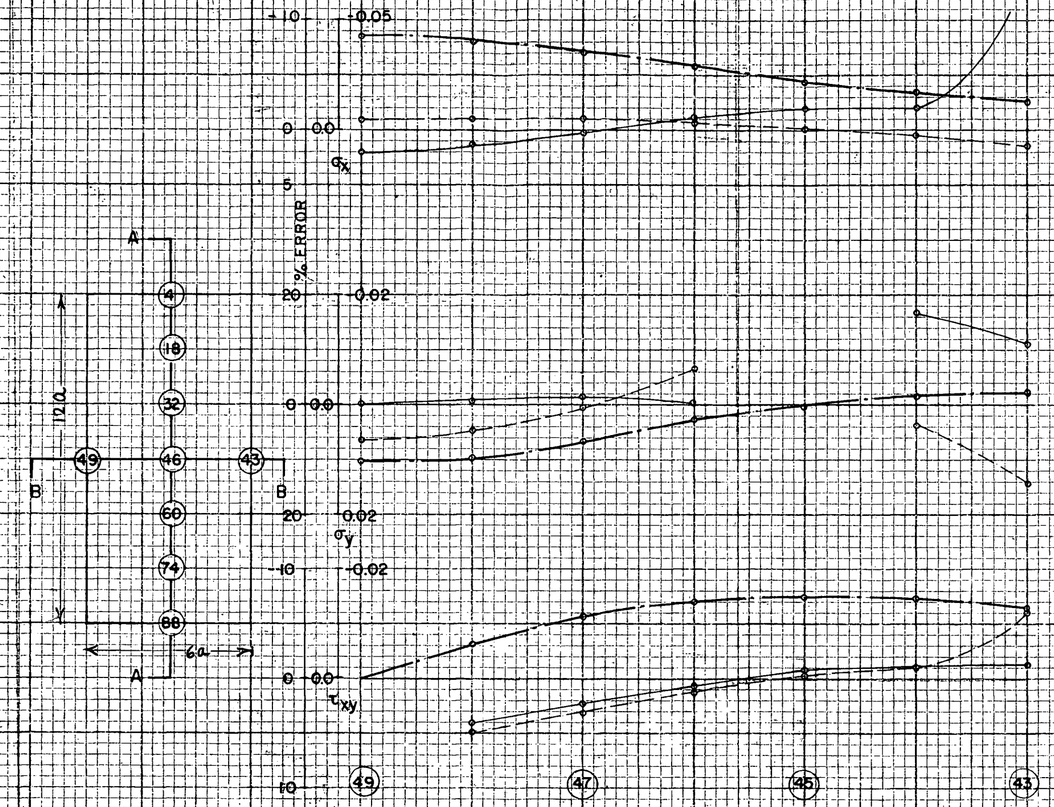

RESULTS ALONG SECTION A A

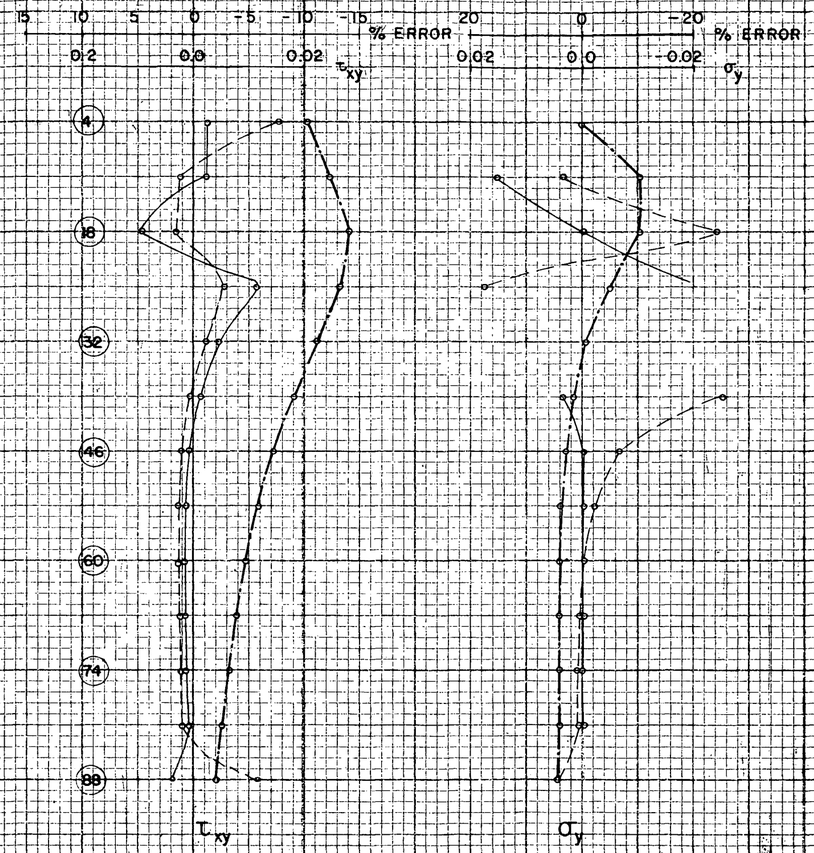

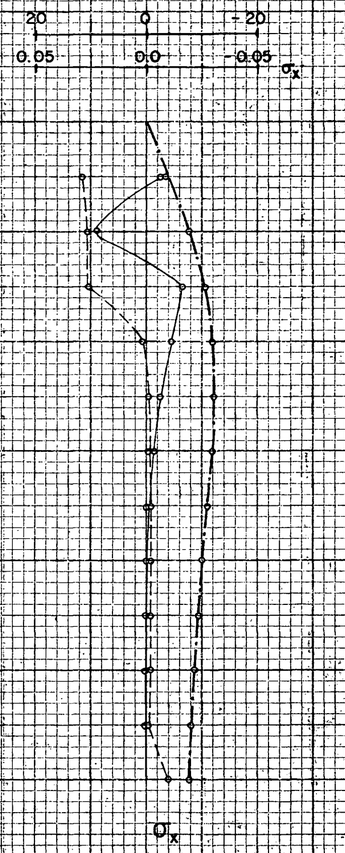

EXAMPLE 2, $\mu = 0.2$

(NO-BAR MODEL)

NOTE

——— % ERROR IN STRESSES OBTAINED FROM NODAL FORCES

– – – – % ERROR IN STRESSES FROM JOINT DISPLACEMENTS

—·—·— ELASTICITY SOLUTION

FIGURES FOR STRESSES TO BE MULTIPLIED BY (P/a)

PLATE - 14

EXAMPLE - 2

NO-BAR MODEL - % ERROR OF STRESSES ALONG AA AND BB FOR $\mu = 0.2$